Toxicity of acute or repeated exposures to particles from pyrotechnic smokes in normal human bronchial epithelial (NHBE) cells 3D culture

Violaine Martin de Lagarde (violaine.delagarde@gmail.com)
Normandie Univ UNIROUEN, UNICAEN, ABTE

Laurence Chevalier
Université de Rouen Normandie, UNIROUEN, INSA Rouen, CNRS, GPM-UMR6634

Clémence Méausoone
Normandie Univ UNIROUEN, UNICAEN, ABTE

Fabrice Cazier
Université du Littoral Côte d'Opale, CCM - Centre Commun de Mesures

Dorothée Dewaele
Université du Littoral Côte d'Opale, CCM - Centre Commun de Mesures

Francine Cazier-Dennin
Université du Littoral Côte d'Opale, UCEIV - Unité de Chimie Environnementale et Interactions sur le Vivant, SFR Condorcet FR CNRS 417

Marion Janona
Normandie Univ UNIROUEN, UNICAEN, ABTE

Cathy Logie
Normandie Univ UNIROUEN, UNICAEN, ABTE

Sophie Achard
Université Paris Cité, Inserm UMR1153 – CRESS, HERA « Health Environmental Risk Assessment »

Véronique André
Normandie Univ UNIROUEN, UNICAEN, ABTE

Tiphaine Rogez-Florent
Normandie Univ UNIROUEN, UNICAEN, ABTE

Christelle Monteil
Normandie Univ UNIROUEN, UNICAEN, ABTE

Cécile Corbière
Normandie Univ UNIROUEN, UNICAEN, ABTE

Research Article

Keywords: Pyrotechnic smoke particles, normal human bronchial epithelial 3D cells, acute and repeated exposures, oxidative stress

Posted Date: November 11th, 2022

DOI: https://doi.org/10.21203/rs.3.rs-2213612/v1

Abstract

Background

Hexachloroethane (HC) based smokes and colored pyrotechnic smokes are widely used in the military field, as screening and signaling smokes, that are reported to cause pulmonary toxic effects in humans and in animal studies. Toxicity of pyrotechnic smokes might be caused by the inhalation of particles that composed the smoke and gives the desired pyrotechnic effect. In a previous study, we showed that smoke particles from a red signaling smoke (RSS) and from an HC obscuring smoke (HC-OS) have an intrinsic oxidative potential and induce an adaptive response in human small airway epithelial cells after an acute exposure. Thus, the aim of this study was to further explore the underlying mechanisms of toxicity linked to oxidative stress response of RSS and HC-OS particles, by using a 3D model of normal human bronchial epithelial cells (NHBE) cultured at the air-liquid interface (ALI).

Results

Acute exposure (24 h) to HC-OS particles induced a weak antioxidant response, characterized by increases of glutathione level and weak increase of one enzymatic antioxidant mRNA expression (*NQO-1*). Acute exposure to RSS particles induced oxidative stress characterized by production of reactive oxygen species (ROS), increases of glutathione level, increases mRNA expression of several enzymatic antioxidants (*SOD-1*, *SOD-2*, *HO-1*, *NQO-1*) and expression of NQO-1 protein as well as increase expression of *IL-8* mRNA. We noticed that 24 h post-exposure to RSS particles, antioxidant response was still induced. Additionally, 24 h post-exposure to RSS particles revealed internalization of particles and morphological changes in 3D NHBE cells like loss of cilia and a cubic epithelium. Repeated exposures to RSS particles on 3D NHBE cells did not induce oxidative stress while cubic changing aspects of 3D NHBE cells were observed.

Conclusions

Thus, although further studies are needed to understand the mechanisms underlying these cubic changes, these results revealed differences in toxicity responses between the two types of particles, characterized by an RSS particles-induced oxidative stress as well as morphologic changes. Overall, this study provides a better overview of the toxic effects of pyrotechnic smoke particles whose toxic risks were very little studied.

Background

Pyrotechnics are defined by the area of technology that deals with the application of self-contained and self-sustained exothermic chemical reactions of solids to produce heat, light, sound, smoke, motion, combinations of these, and/or useful reaction products (Kosanke et al., 2013). Pyrotechnics are very well

known in form of fireworks displays, a major source of entertainment on holidays and special events all over the world. A major use of pyrotechnics is the military field for the production of light, ignite devices used in the artillery and production of smokes for signaling and obscuring or screening, in operations or for the training of soldiers. Pyrotechnics smokes are a complex mixture of several compounds including an oxidizer, a reducing agent which is the fuel, a dye for colored smokes and various other additives, generating an aerosol, composed of gas and particles in suspension, allowing the desired pyrotechnic effect (Hemmilä, Hihkiö, & Linnainmaa, 2007).

The most commonly screening smoke used is one based with hexachloroethane (HC) and a metallic fuel, usually zinc (Zn) (Conkling & Morcella, 2018), generating a greyish-white smoke ($ZnCl_2$) with excellent hiding capacity. Exposure to HC/Zn based smoke on soldiers is reported to cause mucosal irritation, coughing, sore throat, nausea, and vomiting, within the several hours to one day, followed by a second wave of respiratory inflammation (dyspnea, cough, fever, and malaise) taking up to several weeks to abate (El Idrissi et al., 2017). Delayed inflammatory response may trigger by inhaled $ZnCl_2$ particles (El Idrissi et al., 2017). In some cases, in confined spaces, exposure to $ZnCl_2$ smoke can lead to death (Holmes, 1999; Macaulay & Mant, 1964; Pettilä et al., 2000). *In vivo* studies are in line with those symptoms observed in humans (National Research Council (U.S.), 1997). For signaling purposes a diversity of colored smokes are used, composed of an organic dye generally from the anthraquinone family. Toxicity of exposure to colored smokes have never been reported in humans except for individual dyes that showed to cause skin irritation (National Research Council (U.S.), 1999). *In vivo* studies on aerosol generated by various colored smokes showed pulmonary irritations (salivation, dyspnea up to seven days after exposure) and damages like pulmonary necrosis, mucosa desquamation, alveolar oedema, chronic pneumoniae or pulmonary inflammation (National Research Council (U.S.), 1999). More recently, a report realized in rats of a red smoke composed of 1-isopropylamino-anthraquinone showed that repeated exposures caused hyperplasia of the nasal epithelium, sometimes accompanied by degeneration of the nasal mucosa (Crouse et al., 2017). These nasal lesions had disappeared after 4 weeks of rest.

The cellular mechanisms underlying the respiratory toxicity of colored and HC based smokes have been little studied (Hemmilä et al., 2010, 2013; Hemmilä, Hihkiö, Kasanen, et al., 2007; Hemmilä, Hihkiö, & Linnainmaa, 2007; van Hulst et al., 2013). HC-based smokes like HC/Zn or HC/Zn/2,4,6-trinitrotoluene (TNT) have been reported to strongly reduce cell viability and have genotoxic effects on BEAS-2B cells (Hemmilä et al., 2010; Hemmilä, Hihkiö, Kasanen, et al., 2007). Colored smoke is often composed of mixtures of dyes whose proportions may vary from one manufacturer to another. Depending on their chemical composition, colored smokes can have cytotoxic and genotoxic effects on BEAS-2B and A549 cells (Hemmilä et al., 2013; Hemmilä, Hihkiö, & Linnainmaa, 2007; van Hulst et al., 2013). However, the pathophysiological mechanisms of combustion products from pyrotechnic smokes inducing pulmonary toxicity remains unclear.

Beside the risks of explosion and the direct inhalation of gas, toxicity of pyrotechnic smokes can come from the inhalation of particles. Thus, occupationnal exposure toxcity of pyrotechnic smokes of military

personnel have been rising concerns about the health risks associated with their use. Short term exposure is often indicated to cause irritation of the upper respiratory tract and also affects deeper airways, but there are still many uncertainties about the severity of these health effects, particularly after repeated exposures. It is well known that toxicity of air pollution particles have been linked to their small size allowing to reach distal lung region (Kwon et al., 2020; Terzano et al., 2010) and by their complex chemical composition of ions, metals, organic compounds and biological contaminants (Kelly & Fussell, 2015; Steenhof et al., 2011). According to the smoke type, the particles emitted have various sizes, with an aerodynamic diameter < 5 µm (Karlsson et al., 1991), or < 2 µm (Hemmilä et al., 2013; van Hulst et al., 2017), or < 1µm (Hemmilä, Hihkiö, & Linnainmaa, 2007), or < 400 nm (Martin de Lagarde et al., 2022). Our previous study showed that smoke particles from a red signalling smoke (RSS) or an hexachloroethane-based obscuring smoke (HC-OS) are highly concentrated in ions (NO_3^- K^+, Cl^-), in metal elements (Al, Ba, Ca, Cu, Fe, K, Mg, Na, S, Sb, Sn, Zn,) and contain numeroius organic components (quinones, chlorinated organic components and polycyclic aromatic hydrocarbons (PAHs) like naphtalene derivatives) (Martin de Lagarde et al., 2022). The results from this study demonstrated that the both types of smoke particles have an intrinsic oxidative potential and were able to induce both antioxidant and inflammatory responses in primary Small Airway Epithelial Cells (SAEC) cultured at Air-Liquid Interface (ALI) according to the particle composition. The particle-mediated antioxidant response, associated with inflammation, is a well-known mechanism of oxidative stress that could lead to damage the airway epithelium (Falcon-Rodriguez et al., 2016; Sethi et al., 2019). 3D airway models such as normal human bronchial epithelial cells (NHBE) grown at ALI exhibiting a pseudostratified epithelium with a mucociliary function (Bérubé et al., 2010; Boublil et al., 2013; Juarez-Facio et al., 2022; Rayner et al., 2019) appear to be very relevant to study particle toxicity. Moreover, this model allows to study internalization of particles and structural changes of the pulmonary epithelium both after acute and repeated exposures (Aufderheide et al., 2015; Boublil et al., 2013; Ghio et al., 2013; Platel et al., 2020; Sotty et al., 2019).

Thus, the aim of this study was to explore the oxidative stress mediated by RSS and HC-OS particles, that are complex chemical mixture, on a 3D model of NHBE cells. Cytotoxicity, Reactive Oxygen Species (ROS) production, antioxidant and inflammation markers were analysed. Moreover, we investigated the morphological changes of the airway epithelium and the fate of smoke particles.

Results

Cell Viability After 24 H Exposure To Particles

Cell viability of 3D NHBE cells after 24 h of exposure to RSS particles or HC-OS particles was evaluated by MTT assay, measurement of ATP levels (**Table 1**) and by exploration of cells distribution in cell cycle phases (**Supp data, Table S1**). No changes in cell viability for all the concentrations tested was observed for both types of particles whatever the viability methods used.

Table 1: Cell viability after 24 h exposure to RSS or HC-OS particles (6.25 12.5 ; 25 ; 50 µg/cm^2). MTT assay : results are presented as percentage of cell viability compared to the control (cells cultured with

PBS). ATP: results are expressed as ratio relative to the control (cells cultured with PBS). Data were expressed as mean value ± SD (n ≥ 3).

	RSS particles		*HC-OS particles*	
Concentration (µg/cm²)	**% cell viability** (MTT assay)	**ATP (fold change)**	**% cell viability** (MTT assay)	**ATP (fold change)**
0	100 ± 4	1 ± 0.2	100 ± 5	1 ± 0.2
6.25	93 ± 8	0.95 ± 0,1	92 ± 5	1.0 ± 0.04
12.5	101 ± 3	0.97 ± 0.1	91 ± 5	1.1 ± 0.16
25	96 ± 6	0.82 ± 0.2	89 ± 1	1.1 ± 0.18
50	105 ± 6	0.91 ± 0.1	98 ± 5	1.0 ± 0.19

Oxidative stress markers after 24 h of exposure to particles

ROS production

Reactive Oxygen Species (ROS) production was measured using Mitosox probe. First, 1 h and 4 h of exposure to RSS particles showed rapid production of ROS at all concentrations tested (1.2- to 1.6-fold) (Fig. 1A) while HC-OS particles were not able to induce a ROS overproduction (Fig. 1B). Additionnally, 24 h of exposure to RSS particles induced ROS production with the three highest concentrations tested by 1.2- to 1.6-fold (Fig. 1C).

Glutathione levels after 24 h of exposure to particles

In order to explore the antioxidant response, the total glutathione concentration was measured (Fig. 2). After 24 h of exposure to RSS particles, results showed a trend for the glutathione ratio to increase in a dose-dependent manner but the increase is only significant at the concentration of 50 µg/cm^2 (1.5-fold). A significant increase of total glutathione level by 1.4-fold was observed after 24 h of HC-OS particles exposure at 25 µg/cm^2 and 50 µg/cm^2 (Fig. 2).

mRNA and protein expressions after exposure to particles

As shown in Fig. 3, significant upregulations of antioxidant markers after exposure to RSS and HC-OS particles were observed. RSS particles exposures caused a moderate induction of *SOD-1* (25 and 50 µg/cm^2) and *SOD-2* (50 µg/cm^2) mRNA expression by 1.4 fold (Fig. 3A). We showed a greater over expression dependant of particle concentrations for *HO-1* (12.5 µg/cm^2, 1.8-fold; 25 µg/cm^2, 3.0-fold, 50

µg/cm^2, 8.3-fold) and *NQO-1* mRNA expressions (6.25 µg/cm^2, 2.2-fold; 12.5 µg/cm^2, 2.7-fold; 25 µg/cm^2, 4.1-fold, 50 µg/cm^2, 6.4-fold) (Fig. 3A).

Since antioxidants responses were strongly induced, we investigated the reversibility or delayed responses after 24 h post-exposure to RSS particles. Results revealed that mRNA expressions stayed significantly increased (*NQO-1*: 1.8 to 3.7-fold), were back to normal (*SOD-1*, *SOD-2*, *HO-1*), or still unchanged (*Catalase*) (Fig. 3B).

At protein level, NQO-1 was the only antioxidant protein overproduced after 24 h of exposure to RSS particles at 25 and 50 µg/cm^2 (about 2-fold). After 24 h post-exposure NQO-1 protein expression is induced at all concentrations tested (1.8 to 3.7-fold) (Fig. 3C).

24 h of exposure to HC-OS particles caused only an increased of *NQO-1* mRNA expression by 1.5-fold and 1.7-fold at 25 and 50 µg/cm^2, respectively (Fig. 3D). Given this result, we did not study the mRNA expression after 24 h post-exposure or the expression of proteins.

Il-8 Expression After 24 H Of Exposure To Particles

IL-8 mRNA expression was upregulated at all tested concentrations after 24 h of exposure to RSS particles (Fig. 4A). After 24 h post-exposure to RSS particles, we still observed an increased in *IL-8* mRNA expression but only at 25 and 50 µg/cm^2 (about 2- to 3-fold) (Fig. 4A). 24 h of exposure to HC-OS particles caused an increase of *IL-8* mRNA expression from 25 µg/cm^2 by 2-fold (Fig. 4B).

Epithelium barrier permeability after 24 h of exposure to particles

24 h of exposure to RSS and HC-OS particles did not altered permeability of 3D NHBE cells (**Figure S1**).

Airway Epithelium Integrity Morphology After Exposure To Rss Particles

Since RSS exhibited responses linked to oxidative stress and stronger effects at 50 µg/cm^2 than other concentrations, we decided to further analyze the effects of particle exposure on the morpholgy of the 3D NHBE cells. Control cultures exposed to PBS (control) showed a typical mucociliary pseudostratified epithelium with caliciform and ciliated cells at the apical pole (Fig. 5A). Basal cells showed slight cell-to-cell detachment. After 24 h of exposure to 50 µg/cm^2 of RSS particles, no apparent sign of damages denoted by intracellular vacuoles, or disruption of junction, was revealed compared to the control (Fig. 5B). Cell-to-cell contact seem preserved and no drastic cell detachment were noticed. However, 24 h post-exposure revealed damages with a loss of cilia density associated with some modifications in morphology of apical cells, which appear cuboid with low and regular pale staining with toluidine blue

(Fig. 5D). Additionally, in control conditions, we observed differentiated goblet cells by a bright granular purple stain with toluidine blue and by protruding from the epithelium surface (Fig. 5C**)** while this is not observed in the treated cells (Fig. 5D**)**.

Fate Of Pm After Exposure To Rss Particles

(S)TEM imaging coupled to EDS or EELS was performed to evaluate the fate of RSS particles at 50 µg/cm^2, after 24 h of exposure, on 3D NHBE cells, and to confirm their chemical nature as sourcing from RSS. Figure 6 showed a polar distribution of particles sized dependant: i) submicron fraction was mainly trapped outside the cells at the apical pole and exhibited a complex chemical composition associating major and minor compounds of RSS particles (Fe, Al, Si, S, Mg, Ca) (Fig. 6A). ii) Location of nanoranged particles was found into apical cells in the form of small cluster or isolated with an Fe-rich composition (Fig. 6B). Their presence was also detected in the intercellular space at at the level of the basal cells, meaning the capacity of particles to penetrate into the cells and to reach the basal pole (Fig. 6C).

The most striking results were obtained for the 24 h post-exposure to RSS particles. Wide field scanning observations using backscattered electrons gave an overview of the particles behavior and confirmed the events described previously. Figure 7A revealed the accumulation of heavy elements in large number of intracytoplasmic compartments. Large aggregates (~ 350 nm) of iron rich particles (Fig. 7D **blue arrows)** were detected inside vacuolar compartment of apical cells, as well as isolated nanometric particles (~ 10 nm) (Fig. 7G **orange arrows**). In addition, inside compartments, particles seemed frequently associated with an homogeneous gentle-dense electron material, that the feature in EM are typical of mucin (Fig. 7C). Chemical analysis identifies mostly the presence of iron (Figs. 7B, E **and G)**

Cell viability after repeated exposures to RSS particles

Since 24 h of exposure to RSS particles induced stronger cell responses than HC-OS particles, we performed repeated exposures to RSS particles to further explore their toxicity. 3D NHBE cells were exposed to a dose that caused effects after acute exposure (12.5 µg/cm^2) and a lower dose (3.125 µg/cm^2). Repeated RSS particles treatments (16 h exposure / days during 4 days) showed a weak but significant increase at 12.5 µg/cm^2 in cell viability compared to PBS control (106 ± 1 vs 100 ± 4, P = 0.0079) (Table 2). However, ATP content (Table 2) and distribution of cells in cell cycle (**Table S2**) were not modified.

Table 2
Cell viability after repeated exposures to RSS particles (3.125 ; 12.5 µg/cm^2). MTT assay : results are presented as percentage of cell viability compared to the control (cells cultured with PBS). ATP (fold change): results are expressed as ratio relative to the control (cells cultured with PBS). Data were expressed as mean value ± SD (n ≥ 3). **p ≤ 0.01

	RSS particles	
Concentration (µg/cm^2)	**% cell viability (MTT assay)**	**ATP (fold change)**
0	100 ± 4	1.0 ± 0.5
3.125	93 ± 8	0.95 ± 0.06
12.5	**106 ± 1****	0.91 ± 0.3

Oxidative stress and inflammation responses after repeated exposures to RSS particles

Repeated exposures to RSS particles did not modify concentration of total glutathione (Fig. 8A) and only induced *NQO-1* mRNA expression by 2.0 fold at 3.125 µg/cm^2 and 3.0-fold at 12.5 µg/cm^2 (Fig. 8B). In addition, repeated exposures to RSS particles had no effect on *IL-8* mRNA expression (Fig. 8C).

Epithelium barrier permeability after repeated exposure to RSS particles

After repeated exposure to RSS particles, surprisingly we observed a slight but significant decrease of dextran fluorescence at the basal side. This decrease was observed with the both concentrations and was weakly and significantly observed at the higher concentration tested (p = 0.0286) (Fig. 9), reflecting decrease of membrane permeability.

Effect on epithelium morphology after repeated exposures to RSS particles

Since decrease of permeability of the epithelium was observed after repeated exposures to 12.5 µg/cm^2 of RSS particles, we further analysed morphological changes of 3D NHBE cells to this concentration. The impact of the repeated exposures on the morphology are mainly characterized by the changes in cuboid aspect of the epithelium (Fig. 10B) compare to control (Fig. 10A).

Fate of PM after repeated exposure to RSS particles

Electron microscopy analysis of repeated exposures sample, exhibits similar results as observed for post-exposure. Large aggregates constituted of nanosized spherules (around 10 nm) are observed inside apical cells (Fig. 11A), located in vacuolar compartments and are frequently associated to single or

individualized particles (Fig. 11B). The chemical analysis of such nanoparticles stay difficult mainly because of the very low signal emitted by particles. To override those limitations, the acquisition time is highly increased with the adverse effect to damage the sample. However, we revealed by electron loss spectrometry, the Fe-rich composition of particles internalized as observed previously for the post-exposure. In addition we detect Ca-associated to particles.

Discussion

In our previous study, we showed that RSS and HC-OS particles have an intrinsic oxidative potential and an ability to induce antioxidant and inflammatory responses in SAEC model (Martin de Lagarde et al., 2022). With the aim of getting closer to the human *in vivo* conditions, here we used NHBE cells grown at ALI during 14 days that formed a pseudo-stratified mucociliary epithelium (Juarez-Facio et al., 2022). Acute and repeated exposures to smoke particles were performed to further explore the underlying mechanisms of toxicity, in particular oxidative stress response of pyrotechnic smoke particles.

24 h of exposure to RSS and HC-OS particles did not affect cell viability, which is in line with our previous study in SAEC (Martin de Lagarde et al., 2022). Other studies on total aerosol generated by red smokes and HC based smokes reported to cause decrease in cell viability of BEAS-2B and A549 cell lines, 24 h and 48 h after exposure (Hemmilä et al., 2010, 2013; Hemmilä, Hihkiö, Kasanen, et al., 2007; Hemmilä, Hihkiö, & Linnainmaa, 2007; van Hulst et al., 2017). Our tested concentrations appeared to be non-cytotoxic. It is very difficult to compare our concentrations regarding cytotoxicity with the studies mentioned above since the concentrations were either defined in quantity of burnt smoke (g), in density (g/m^3), or only in number of burnt grenades. However, concentrations used in this work are consistent with other studies assessing the particle toxicity using pulmonary cell models cultured at ALI conditions, and where concentrations between 7 and 45 $\mu g/cm^2$ were used (Abbas et al., 2019; Lan et al., 2021).

Our results showed that RSS particles induced ROS production after 1 h, 4 h and 24 h of exposure in a dose-dependent manner. PM-induced ROS formation have been reported in other pyrotechnic activities like fireworks (Hickey et al., 2020) or firearms (Bergström et al., 2015). Unexpectedly, HC-OS particles were not able to produce ROS while they are extremely rich in metals like Fe (12.1 mg/g) (Martin de Lagarde et al., 2022) which is known to induce ROS formation (Jin et al., 2019; Xu et al., 2020). RSS particles displayed the highest organic fraction (quinones and polycyclic aromatic hydrocarbons, PAHs) while HC-OS particles contained chlorinated aromatic or polyaromatic compounds (Martin de Lagarde et al., 2022). The implication of organic compounds like PAHs in a greater ROS production is showed in several studies (Ekstrand-Hammarström et al., 2013; L. Jin et al., 2019; J. Li et al., 2021; Longhin et al., 2013). Total glutathione level, antioxidant mRNA and protein expression were analyzed after 24 h of exposure to smoke particles in 3D NHBE cells. In line with the production of ROS, RSS particles showed an induction of antioxidant defenses by increasing level of total glutathione, expressions of mRNA *SOD-1*, *SOD-2*, *HO-1*, *NQO-1* and expression of NQO-1 protein. HC-OS particles showed a weak antioxidant response by increasing level of total GSH and the expression of mRNA *NQO-1*. In other studies, a 24 h of exposure to PM like $PM_{2.5}$ (Niu et al., 2020; Zhao et al., 2020) or PM_{10} (Chirino et al., 2010) induced a decrease in total

glutathione concentration in pulmonary cells. In our study, we could presume that total glutathione firstly reacts with ROS produced at 1 h and 4 h of exposure to RSS particles and then overproduced to be restored and acts against prolonged exposure to RSS particles. For example, 3 h post-exposure to ultrafine particles reduced total glutathione level but is followed by an increase after 24 h post-exposure in BEAS-2B cells (Juarez Facio et al., 2022). However, the concentration increases of total glutathione after 24 h of exposure to HC-OS particles at 25 and 50 µg/cm^2 remain very unclear while no ROS production was observed at 1 and 4 h of exposure. Because of the pleiotropic roles of glutathione in the cell (Hatem et al., 2017; Merk et al., 2020), it remains difficult to attribute this result to oxidative stress alone, which should be assessed by measurements of the GSH/GSSG ratio. SODs and catalase are the first line of intracellular antioxidant enzymes, SODs convert $O_2Ÿ^-$ to H_2O_2, and catalase reduces H_2O_2 to H_2O (Ighodaro & Akinloye, 2018). The increases of mRNA *SOD-1* and *SOD-2* by 24 h of exposure to RSS particles are in line with the $O_2Ÿ^-$ production measured. The induction of *SOD* expression is in line with other works on particles (Abbas et al., 2019; Fernando et al., 2019; Juarez Facio et al., 2022). HO-1 is an important cytoprotective enzyme that is highly upregulated by a number of stimuli like heme, nitric oxide, heavy metals, growth factor, cytokines, modified lipids and others (Loboda et al., 2016). Its expression is often overproduced after exposure to PM (Crobeddu et al., 2017; Deng et al., 2013; Fernando et al., 2019; Frias et al., 2020; Juarez-Facio et al., 2022; Niu et al., 2020; Skuland et al., 2017) which is similarly observed with a 24 h of exposure to RSS particles. NQO-1 antioxidant marker was highly induced at mRNA and protein levels by RSS particles even after 24 h post-exposure. Since NQO-1 is very well known to be induced by quinones catalyzing their reduction (Burchiel et al., 2007; Dinkova-Kostova & Talalay, 2010), the strong upregulation of *NQO-1* is very probably related to the anthraquinones that composed the red dye of RSS particles (Martin de Lagarde et al., 2022). Indeed, anthraquinones can count approximately for 40% of the total composition of red coloring smokes (National Research Council (U.S.), 1999). Additionally, this upregulation of NQO-1 could drive an excessive production of $O_2Ÿ^-$ by the redox cycling of quinones (Valavanidis et al., 2013; Zheng et al., 2020). A very recent study developed a model of quantitative structure activity relationship to predict the health risks of an acute exposure to anthraquinones dyes used in the military field (Dilger et al., 2022). High to very high toxicities were predicted for acute inhalation, genotoxicity, mutagenicity, endocrine disruption and development.

According to the hierarchical stress response model, increase of oxidative stress can lead to inflammation and finally to cytotoxicity and initiation of programmed cell death (Araujo & Nel, 2009; Peixoto et al., 2017; Xiao et al., 2003). Upregulation of the pro-inflammatory marker *IL-8* by RSS particles after 24 h of exposure and 24 h of post-exposure was observed. This induction was in accordance with exposure to particles from other pyrotechnic activities like firearms (Bergström et al., 2015) or to combustion-derived particles (Juarez-Facio 2022). To confirm the induction of inflammation by RSS particles, secretion of IL-8 and other pro-inflammatory markers, like TNF-α, IL-1β or IL-6, need to be analyzed (Sotty et al., 2019). Overall, results of acute toxicity showed that RSS particles were able to induce an oxidative stress and an inflammatory response which were similarly observed in our previous work, while HC-OS particles had less effects in 3D NHBE cells compared to SAEC (Martin de Lagarde et al., 2022).

Since 3D culture of NHBE cells at ALI highly developed a mucociliary clearance (Juarez-Facio et al., 2022; Rayner et al., 2019; Sotty et al., 2019), we analyzed the morphological changes of the airway epithelium and the fate of RSS particles. At the resolution of light microscopy, no apparent displayed sign of damage denoted by intracellular vacuoles, or disruption of junction, was revealed on cultures exposed 24 h to 50 µg/cm^2 of RSS particles. The extension of 24 h post-exposure favors the morphology changes into a cuboid epithelium and a trend in loss of ciliature. Severe ciliatoxicity with a decrease of number and length of cilia were observed after repeated exposure to cigarette smoke on differentiated NHBE cells (Aufderheide et al., 2015; Brekman et al., 2014). Changes in airway epithelium structure may be related to oxidative stress mediated by RSS particles as suggested by Falcon-Rodriguez et al. (2016). Electron Microscopy investigations highlighted the capacity of particles to be internalized into cells and to be stored in compartment. After 24 h of exposure to RSS particles at 50 µg/cm^2, cluster of particles were mainly trapped outside the cells, in the mucus, while some nanoparticles were found into the apical cells. Mucus is the first protective layer of bronchial epithelium to external aggression and NHBE differentiated model is well known to secrete mucus (Rayner et al., 2019) acting as a filtering barrier according to the size or the surface-charge of particles. After 24 h post-exposure, we showed more internalization of numerous nanoparticles into vacuoles in the apical cells. These observations are coherent with the study of Boublil (2013) who have demonstrated the capability of 3D NHBE cells to internalize and accumulate $PM_{2.5}$ after repeated exposures in the basal and apical cytoplasm of the cells (Boublil et al., 2013). Internalization of $PM_{2.5}$ into vacuoles was also observed in BEAS-2B cells (Dornhof et al., 2017) or SAEC cells (Lan2021) and with gunshot particles in A549 cells (Bergström et al., 2015). It is well agreed that the diffusion rate through mucus layer decreases with increasing particle size (García-Díaz et al., 2018), allowing internalization of only nanometer particles which are consistent with our results. In addition, we observed the presence of calcium associated to the particles that might be attributed to mucin content. Paz et al., (2003) reported that calcium is necessary to keep mucins condensed and packed in intracellular granules under physiological conditions (Paz et al., 2003). The microscopy results obtained in this study highlight a putative interaction of RSS particles with secreted mucins, conditioning their fate in bronchial epithelium.

In order to be closer of a military occupational exposure, we analyzed RSS particles toxicity after repeated exposures (4x16 h/day) to lower doses than acute exposure. Exposure of 16 h could be considered as a long time of exposure but it could represent a residual particles deposition in the lower respiratory tract (Geiser & Kreyling, 2010; Lan et al., 2021). Since antioxidant and inflammatory markers were still induced 24 h post-exposure to RSS particles, internalization of particles were more pronounced and important changes in the airway epithelium were observed after this recovery time, we expected to have more harmful effects after repeated exposures. However, we showed only induction of *NQO-1* mRNA at the two tested concentrations. Total glutathione content and *IL-8* mRNA expression were not modified. The main result is the change in the organization of the epithelium to a pseudostratified into a cuboid epithelium, which seems more pronounced than 24 h post-exposure. These morphological changes could be related to the decrease of the permeability of the epithelium barrier that was observed by measuring the passage of Dextran-FITC and by the increase of MTT reduction, suggesting a cell proliferation or a metabolic

activation. However, most studies showed that particles caused other types of morphological alterations like a change in spindle shape and the formation of paracellular holes (Dornhof et al., 2017), structural and functional damage to mitochondria (X. Jin et al., 2018; N. Li et al., 2003), or disturbances in membrane integrity (Caraballo et al., 2011; Dong et al., 2020; Lin et al., 2021). Thus, the mechanisms underlying these cubic changes are very unclear since no oxidative stress was observed at the time point studied. However, oxidative stress linked to an inflammatory response could occur transiently during repeated exposures, which could lead to morphological modifications. Therefore, a kinetic analysis of the antioxidant response seems necessary for this type of exposure. Moreover, in our 3D model, it was evidenced that particles were trapped into cytoplasmic vacuoles and probably linked to mucins. In addition, we observed hypersecretion of mucus after repeated exposures but we did not quantify this phenomenon. Quantification of mucins as well as study of the proportion of goblet, ciliated and basal cells should be performed to clarify the underlying mechanisms.

Conclusion

In conclusion, the aim of this study was to explore toxicity of particles from two different pyrotechnic smokes and to better evaluate the underlying mechanisms of biological responses by using 3D NHBE cells. Our results demonstrated an induction of oxidative stress by RSS particles after acute exposure, characterized by a ROS production and increases of antioxidant and pro-inflammatory markers, while HC-OS particles were less harmful. Additionally, RSS particles were internalized into cells and generated cell morphological changes, highlighted that 3D NHBE cells is a very relevant model to study the fate of particles and the changes of the airway epithelium that might be occurs after particle exposure. Finally, repeated exposures to RSS particles did not induce oxidative stress at the time point studied while metabolic activation and changes in the appearance of the epithelium were observed. Thus, further investigations need to be performed to understand these results. Overall, this study provides a better overview of the acute and repeated toxic effects from pyrotechnic smokes particles whose toxic risks were very little studied. Research methodology developed here could be used to study other colored smokes containing anthraquinones dyes or new formulation of smokes.

Material And Methods

Particle Sampling

Particles from RSS and HC-OS were collected on cascade impactors and prepared for particles suspensions as previously described in (Martin de Lagarde et al., 2022).

3d Nhbe Cell Culture And Particle Treatments

Primary NHBE cells (ATCC, USA) were obtained from biopsy isolated from a healthy donor. Firstly, the cells were grown for 5 days in T-75cm^2 flasks with Airway Epithelial Cell Basal Medium (ATCC, USA),

supplemented with the Bronchial Epithelial Cell Growth Kit (ATCC, USA) and 0.1% (v/v) penicillin/streptomycin (10 Units/mL; GIBCO, USA). Between 70 and 80% confluency, NHBE cells were trypsinized and seeded at 90 000 cells/insert on transwells polyester permeable membrane cell culture inserts (12 mm diameter, pore size 0.4 µm, Costar, Corning®) pre-coated with a 30 µg/mL collagen solution (Rat Tail Collagen Type 1, Corning®) in PBS for 1 hour at 37°C. At confluence, cells were placed under Air-Liquid Interface (ALI) conditions by removing the apical medium and replacing the basal medium by PneumaCult-ALI Basal Medium (STEMCELL Technologies, Canada) supplemented with PneumaCult-ALI 10X Supplement, PneumaCult-ALI Maintenance supplement 100X (ATCC, USA) and hydrocortisone (2 µmol/L) (STEMCELL Technologies, Canada). ALI culture was maintained for 14 days, allowing progressive differentiation of cells into ciliated, goblet and basal cell types within a pseudo-stratified epithelium (Juarez-Facio et al., 2022). The cells were maintained at 37°C in 95% humidified air with 5% CO_2 and the medium was changed every two days. Three days before expsoure, mucus production was removed by gentle rinsing with medium.

After 14 days of culture at ALI conditions, the exposures were performed by directly deposing particle suspensions of RSS and HC-OS (0.2 mL) on the apical side of cells at 37°C in a humidified 5% CO_2 atmosphere. 3D NHBE cells were exposed to smoke particles for 1 h, 4 h or 24 h (6.25, 12.5, 25 and 50 µg/cm^2). At the end of exposure, the apical side of the epithelium was rinsed with PBS and cells were collected. To study responses reversibility or delayed responses, an additional condition corresponding to an incubation of 24 hours post-exposure was carried out. A repeated exposure protocol was also performed with four successive particle treatments of 16 h per day (3.125 and 12.5 µg/cm^2). As reference control, cells were exposed to 0.2 mL of PBS under the same conditions. Cells maintened in ALI conditions are also used as reference air control.

Cell Viability Assay

3D NHBE cells viability was determined using the MTT assay 24 h of exposure to particles and repeated exposures to RSS particles. Briefly, after exposure, 50 µL of MTT reagent (5 mg/mL) was added to basal medium and incubated for 3h at 37°C. After incubation, dimethyl sulfoxide (DMSO) was added on each transwell and mixed thoroughly. The optical density at 570 nm was measured with a microplate reader (SAFAS Xenius, Safas, Monaco). Results are expressed as % viability = (Absorbance in the sample / Absorbance in the control PBS) x 100. Data were expressed as mean value ± SD of at least three independent experiments.

Cell Cycle Analysis By Flow Cytometry

Cell cultures atfter 24 h of exposure to particles and repeated exposures to RSS particles were dissociated with trypsin–EDTA, resuspended, fixed and permeabilized with ethanol (70%) for 30 min at 4°C. Resulting samples were spun down and resuspended in 0.5 mL of FxCycle™ PI/RNase Staining Solution (Thermofisher, France) stain to each flow cytometry sample for 20 min. Cells were then analysed by flow

cytometry (Attune's Next, Thermofisher, France) with ten thousand events analysed per sample. Results are expressed as % of cells in each phases of cell cycle.

Atp Level

Extraction and measurement of ATP level, after 24 h of exposure to particles and repeated exposures to RSS particles, by high performance liquid chromatography coupled with a diode array detector (HPLC-DAD, 1260 Infinity II, Agilent Technologies) were realized as préviously described in (Juarez-Facio et al., 2021). Results are expressed as ratio relative to the control.

Ros Production

Intracellular Reactive Oxygen Species (ROS) generation was assessed using the fluorescent MitoSox Red Mitochondrial Superoxyde Indicator (Invitrogen, France) probe dissolved in dimethyl sulfoxide (DMSO) at 5 mM diluted to 10 µM in PBS. After 1 h, 4 h or 24 h of exposure to particles, cells were washed and were incubated with the probe (0.2 mL per insert) for 10 min at 37°C. Cells were then washed twice with PBS and fluorescence was measured at 580 nm on a microplate reader Spark® (TECAN Trading AG, Switzerland). Results are expressed as ratio relative to the control.

Total Glutathione Quantification

Total glutathione quantification was performed from supernatants obtained from ATP quantification, after 24 h of exposure to particles and repeated exposures to RSS particles. Briefly, 20 µL of the sample, 20 µL of buffer (160 mM $Na_2H_2PO_4$; 8 mM EDTA, pH 7.4), 200 µL of buffer reagent and 40 µL of glutathione reductase (8.5 U/mL) were deposed in a 96 well plate. Absorbance was measured at 405 nm for 2 min and 40 s. The reagent buffer consisted of NADPH (0.4 mM), DTNB (1 mM) and methanol (10%) (VWR, France) in buffer. Glutathione concentrations were determined from a standard curve and normalized to protein content (Lowry assay). Results are expressed as ratio relative to the control.

Mrna Expression Measurements By Quantitative Real Time Rt-pcr

Total RNA was isolated from cells using TRI-REAGENT® (Sigma-Aldrich, France) according to the manufacturer's instructions. The "AffinityScript QPCR cDNA Synthesis Kit with OligodT" (Agilent Technologies) was used to reverse transcribe mRNA in each sample into cDNA, and quantitative real-time PCR (qPCR) was performed to determine the transcript levels of the target genes' transcript with the "Brilliant III Ultra-fast SYBR Green QPCR Master Mix" (Agilent Technologies) using a thermocycler (Stratagene Mx3005P, Agilent Technologies). β2M was used as the internal reference gene and the relative expression of superoxyde dismutase – 1 (SOD-1) and – 2 (SOD-2), Catalase, heme oxygenase-1 (HO-1), NAD(P)H quinone dehydrogenase-1 (NQO-1) and interleukine-8 (IL-8) were calculated using the

$2^{-\Delta\Delta Ct}$ method (Livak & Schmittgen, 2001). mRNA markers were measured after 24 h of exposure to particles, 24 h post-exposure to RSS particles and after repeated exposures to RSS particles.

Western Blot

Proteins were extracted after 24 h of exposure to RSS particles and 24 h post-exposure. Extraction was performed with RIPA Lysis Buffer (Merck) diluted 1:10 in ultra pure sterile water supplemented with Phosphatase and Protease Inhibitor Cocktail 100X (Thermofisher Scientific, France) at 4°C. Protein quantification was made with the Bradford protein assay. 12 µg of proteins per sample were separated in 10% TGX Stain-Free polyacrylamide gel (Bio-Rad Laboratories, France) using Mini-PROTEAN® Tetra Cell (Bio-Rad Laboratories) and transferred to nitrocellulose membranes (Amersham Protran 0.45 NC) using Trans-Blot® Turbo™ Transfer System (Bio-Rad Laboratories). Primary antibodies against various proteins, Catalase (Novus Biologicals, California, USA), MnSOD (Aviva System Biology, Clinisciences, France), CuZnSOD (Cusabio, Clinisciences, France), NQO-1 (St John's Laboratory, London, UK), HO-1 (BioVision, Clinisciences, France), β-actin (Sigma-Aldrich, Missouri, USA), were used after having been diluted, and their binding was detected using Peroxidase AffiniPure Donkey Anti-Mouse IgG (H + L) or Peroxidase AffiniPure Goat Anti-Rabbit IgG (H + L) (Jackson ImmunoResearch Europe, UK) followed by enhanced chemiluminescence reagents (Bio-Rad Laboratories). Antibodies against GAPDH (Cell Signalling Technology, Massachusetts, USA), as internal control, was also used. The results were analyzed with a ChemiDoc Imaging System (Bio-Rad Laboratories). Results are expressed as ratio relative to the control.

Epithelium Barrier Permeability

After 24 h of exposure to particles and repeated exposure to RSS particles, fluorescein-5-isothiocyanate (FITC)-dextran 70 kDa (Sigma-Aldrich) was applied to the apical side of cells and incubated for 2 hours at 37°C. After washing the cells, fluorescence was measured in the culture medium at the basal side after removing transwell at 535 nm on a microplate reader Spark® (TECAN Trading AG, Switzerland). Results are expressed as ratio relative to the control.

Sample Preparation To Electron Microscopy (Tem) And Scanning Electronic Microscopy (Sem)

Preparation to Electron Microscopy is based on an original EM combined approach involving SEM and TEM observations on a single prepared procedure and is described elsewhere in Chevalier et al., 2022. Briefly, 3D NHBE cells exposed to 24 h to RSS particles (50 µg/cm^2) and 24 h post-exposure as well as repeated exposures to RSS particles (12.5 µg/cm^2) were directly fixed on the Transwell®, 0.4 µm Pore Polyester Membrane Inserts in 2.5% Glutaraldehyde (EMS, USA) in 0.2 mol/L Hepes buffer pH 7.4 (VWR, USA). After several rinses in buffer, membrane inserts were removed from their support and cut in small pieces. Samples were post-fixed in 1% Osmium tetroxide (EMS, USA) for 1 hr at + 4°C and rapidly rinsed

again. Cells were then dehydrated using a graded series of ethanol and acetone before being impregnated with Epoxy Low Viscosity Resin (EMS, USA) under vacuum. The resin was polymerized at 60°C between 48 and 72 hr. For optical microscopy, 800 nm-thin sections were prepared by ultramicrotomy (Ultracut-UCT, Leica-microsystems, Germany) and stained with toluidine Blue (EMS, USA), a metachromatic dye. Observations were performed on an upright light microscope (DM6B, Leica-microsystems, Germany) and images acquired with a sCMOS camera (DFC9000, Leica-microsystems, Germany).

Ultrathin sections (70nm – 80nm) were cut using a UC7 ultramicrotome (Leica-microsystems- Vienna) and placed at once on silicon wafer previously hydrophilized by plasma AR/O2 (RF50W, Ar 35.0 sccm, O2 11.5 sccm) for 4 min (Plasma Cleaner-GATAN- Ametek-USA) for SEM-observations and 400-mesh carbon coated gold-grids for TEM-analysis.

Sem-observations

Serial ultrathin sections <link rid="Sec6">c</link>ollected on wafer were stained for 1 min with a uranyl-less solution (Delta microscopy-France) containing high heavy lanthanum and gadolinium salts, and then were platinum-coated (1 nm) with a precision etching and coating system (PECS-Gatan-Ametek-USA). Electron micrographs were acquired on SEM JEOL 7900 F using the gentle super high-resolution stage bias mode. This function improves high resolution at any accelerating voltage and is particularly well adapted to an insulator biological sample. This mode decelerates the illuminated electron beam and accelerates the electron signal using a biased voltage for the sample (HT 7 kV, probe 2.4 nA, WD 3 mm). Images were obtained with the high ultrasensitive backscattered detector improving Z-contrast at low accelerating voltage.

(S)tem-analysis

Analytical and high-resolution TEM imaging were performed at 80 kV on a JEOL JEM ARM200F (JEOL,Tokyo, Japan) setting with a field emission gun (FEG) and a probe Cs aberration corrector. This TEM is equipped with an energy electron loss spectrometer (GIF- Quantum ER—Gatan-Ametek, USA) upgraded with the Dual EELS option allowing the simultaneous acquisition of two-electron spectra at desired energy. STEM-EDS was also used to investigate the distribution of smoke particles into the 3D NHBE cells. Elemental maps were acquired at 80 kV in STEM mode with an 8C probe size, a camera length of 8 cm, and a 50 µm condenser aperture with an SDD detector XMax TLE (Resolution: 127 ev Mnk 0.7 sr; Oxford-Instruments, Abington, England), with a beam current around 518 pA/cm^2. When the limit of detection was achieved especially for nanometric particle, elemental mapping was performed by energy loss spectrometry as alternative solution. In this case spectra were collected with a 8C probe size, 3 cm length camera, 50 µm condenser lens aperture diameter and 5.0 mm GIF entrance diameter.

Statistical analysis

Results were obtained from at least three independent experiments. Data were analyzed by a non-parametric Mann-Whitney test using GraphPadPrism v9 software. Values of $p \leq 0.05$ are considered to be statistically significant.

Abbreviations

RSS: red signalling smoke; HC-OS: hexachloroethane-based obscuring smoke

Declarations

Acknowledgements

Not applicable

Author contributions

Study design: CC/CMo/DD/FC/FC-D/SA/VA. Data collection: VML/LC/CL/CMé/MJ/TR-F/CC. Data analysis and interpretation: VML/LC/MJ/CC/TR-F/CM. Original draft: VML/LC. Writing, Review and Editing VML/LC/CC/TR-F/SA/VA/CM. All authors reviewed the manuscript

Declaration of Competing Interest

The authors declare that they have no known competing financial interests or personal relationships that could have appeared to influence the work reported in this paper.

Funding

This work was supported by the Agence Nationale de la Recherche Française (ANR Astrid, Grant number: ANR-15-ASTR-0023), and co-supported by the Regional Council of Normandy and the European Union in the framework of the ERDF-ESF (CellSTEM project). Violaine Martin de Lagarde received a PhD fellowship co-funded by the Agence de l'Innovation de Defense (AID) and the Regional Council of Normandy. We thank the Direction Générale de l'Armement (DGA) for technical assistance during use of pyrotechnic smokes and for support in carrying out the study.

Availability of data and materials

The datasets used and/or analysed during the current study are available from the corresponding author on reasonable request.

Ethics approval and consent to participate

Not applicable.

Consent for publication

Not applicable.

Competing interests

The authors declare that there is no competing interests.

References

1. Abbas, I., Badran, G., Verdin, A., Ledoux, F., Roumie, M., Lo Guidice, J.-M., Courcot, D., & Garçon, G. (2019). In vitro evaluation of organic extractable matter from ambient PM2.5 using human bronchial epithelial BEAS-2B cells : Cytotoxicity, oxidative stress, pro-inflammatory response, genotoxicity, and cell cycle deregulation. *Environmental Research*, *171*, 510-522. https://doi.org/10.1016/j.envres.2019.01.052
2. Araujo, J. A., & Nel, A. E. (2009). Particulate matter and atherosclerosis : Role of particle size, composition and oxidative stress. *Particle and Fibre Toxicology*, *6*(1), 24. https://doi.org/10.1186/1743-8977-6-24
3. Aufderheide, M., Scheffler, S., Ito, S., Ishikawa, S., & Emura, M. (2015). Ciliatoxicity in human primary bronchiolar epithelial cells after repeated exposure at the air–liquid interface with native mainstream smoke of K3R4F cigarettes with and without charcoal filter. *Experimental and Toxicologic Pathology*, *67*(7-8), 407-411. https://doi.org/10.1016/j.etp.2015.04.006
4. Bergström, U., Ekstrand-Hammarström, B., Hägglund, L., & Wingfors, H. (2015). Comparing Acute Toxicity of Gunshot Particles, from Firing Conventional and Lead-Free Ammunition, in Pulmonary Epithelial Cell Cultures. *Journal of Toxicology and Environmental Health, Part A*, *78*(10), 645-661. https://doi.org/10.1080/15287394.2015.1017682
5. Bérubé, K., Prytherch, Z., Job, C., & Hughes, T. (2010). Human primary bronchial lung cell constructs : The new respiratory models. *Toxicology*, *278*(3), 311-318. https://doi.org/10.1016/j.tox.2010.04.004
6. Boublil, L., Assémat, E., Borot, M.-C., Boland, S., Martinon, L., Sciare, J., & Baeza-Squiban, A. (2013). Development of a repeated exposure protocol of human bronchial epithelium in vitro to study the long-term effects of atmospheric particles. *Toxicology in Vitro*, *27*(2), 533-542. https://doi.org/10.1016/j.tiv.2012.11.008
7. Brekman, A., Walters, M. S., Tilley, A. E., & Crystal, R. G. (2014). FOXJ1 Prevents Cilia Growth Inhibition by Cigarette Smoke in Human Airway Epithelium *In Vitro*. *American Journal of Respiratory Cell and Molecular Biology*, *51*(5), 688-700. https://doi.org/10.1165/rcmb.2013-0363OC
8. Burchiel, S. W., Thompson, T. A., Lauer, F. T., & Oprea, T. I. (2007). Activation of dioxin response element (DRE)-associated genes by benzo(a)pyrene 3,6-quinone and benzo(a)pyrene 1,6-quinone in MCF-10A human mammary epithelial cells. *Toxicology and Applied Pharmacology*, *221*(2), 203-214. https://doi.org/10.1016/j.taap.2007.02.020
9. Caraballo, J. C., Yshii, C., Westphal, W., Moninger, T., & Comellas, A. P. (2011). Ambient particulate matter affects occludin distribution and increases alveolar transepithelial electrical conductance :

Particulate matter affects alveolar barrier. *Respirology*, *16*(2), 340-349. https://doi.org/10.1111/j.1440-1843.2010.01910.x

10. Chevalier, L., Selim, J., Castro, C., Cuvilly, F., Baste, J.-M., Richard, V., Pareige, P., & Bellien, J. (2022). Combined Electron Microscopy Approaches for Arterial Glycocalyx Visualization. *Frontiers in Cardiovascular Medicine*, *9*, 840689. https://doi.org/10.3389/fcvm.2022.840689
11. Chirino, Y. I., Sánchez-Pérez, Y., Osornio-Vargas, Á. R., Morales-Bárcenas, R., Gutiérrez-Ruíz, M. C., Segura-García, Y., Rosas, I., Pedraza-Chaverri, J., & García-Cuellar, C. M. (2010). PM10 impairs the antioxidant defense system and exacerbates oxidative stress driven cell death. *Toxicology Letters*, *193*(3), 209-216. https://doi.org/10.1016/j.toxlet.2010.01.009
12. Conkling, J. A., & Morcella, C. (2018). *Chemistry of Pyrotechnics Basic Principles and Theory, Third Edition*.
13. Crobeddu, B., Aragao-Santiago, L., Bui, L.-C., Boland, S., & Baeza Squiban, A. (2017). Oxidative potential of particulate matter 2.5 as predictive indicator of cellular stress. *Environmental Pollution*, *230*, 125-133. https://doi.org/10.1016/j.envpol.2017.06.051
14. Crouse, L. C. B., Bazar, M. A., Crouse, C. L., & Januskiewicz, A. J. (2017). *Acute and Subacute Inhalation Toxicity Study in Rats Exposed to Pyrotechnically-Disseminated M18 Red Smoke* (Toxicology study S.0036333-15; p. 403). US Army Research Development and Engineering Command Environmental Acquisition and Logistics Sustainment Program.
15. Deng, X., Rui, W., Zhang, F., & Ding, W. (2013). PM2.5 induces Nrf2-mediated defense mechanisms against oxidative stress by activating PIK3/AKT signaling pathway in human lung alveolar epithelial A549 cells. *Cell Biology and Toxicology*, *29*(3), 143-157. https://doi.org/10.1007/s10565-013-9242-5
16. Dilger, J. M., Martin, T. M., Wilkins, B. P., Bohrer, B. C., Thoreson, K. M., & Fedick, P. W. (2022). Detection and toxicity modeling of anthraquinone dyes and chlorinated side products from a colored smoke pyrotechnic reaction. *Chemosphere*, *287*, 131845. https://doi.org/10.1016/j.chemosphere.2021.131845
17. Dinkova-Kostova, A. T., & Talalay, P. (2010). NAD(P)H:quinone acceptor oxidoreductase 1 (NQO1), a multifunctional antioxidant enzyme and exceptionally versatile cytoprotector. *Archives of Biochemistry and Biophysics*, *501*(1), 116-123. https://doi.org/10.1016/j.abb.2010.03.019
18. Dong, C.-D., Chen, C.-W., Chen, Y.-C., Chen, H.-H., Lee, J.-S., & Lin, C.-H. (2020). Polystyrene microplastic particles: In vitro pulmonary toxicity assessment. *Journal of Hazardous Materials*, *385*, 121575. https://doi.org/10.1016/j.jhazmat.2019.121575
19. Dornhof, R., Maschowski, C., Osipova, A., Gieré, R., Seidl, M., Merfort, I., & Humar, M. (2017). Stress fibers, autophagy and necrosis by persistent exposure to PM2.5 from biomass combustion. *PLOS ONE*, *12*(7), e0180291. https://doi.org/10.1371/journal.pone.0180291
20. Ekstrand-Hammarström, B., Magnusson, R., Österlund, C., Andersson, B. M., Bucht, A., & Wingfors, H. (2013). Oxidative stress and cytokine expression in respiratory epithelial cells exposed to well-characterized aerosols from Kabul, Afghanistan. *Toxicology in Vitro*, *27*(2), 825-833. https://doi.org/10.1016/j.tiv.2012.12.022

21. El Idrissi, A., van Berkel, L., Bonekamp, N. E., Dalemans, D. J. Z., & van der Heyden, M. A. G. (2017). The toxicology of zinc chloride smoke producing bombs and screens. *Clinical Toxicology*, *55*(3), 167-174. https://doi.org/10.1080/15563650.2016.1271125
22. Falcon-Rodriguez, C. I., Osornio-Vargas, A. R., Sada-Ovalle, I., & Segura-Medina, P. (2016). Aeroparticles, Composition, and Lung Diseases. *Frontiers in Immunology*, *7*. https://doi.org/10.3389/fimmu.2016.00003
23. Fernando, I. P. S., Jayawardena, T. U., Kim, H.-S., Lee, W. W., Vaas, A. P. J. P., De Silva, H. I. C., Abayaweera, G. S., Nanayakkara, C. M., Abeytunga, D. T. U., Lee, D.-S., & Jeon, Y.-J. (2019). Beijing urban particulate matter-induced injury and inflammation in human lung epithelial cells and the protective effects of fucosterol from Sargassum binderi (Sonder ex J. Agardh). *Environmental Research*, *172*, 150-158. https://doi.org/10.1016/j.envres.2019.02.016
24. Frias, D. P., Gomes, R. L. N., Yoshizaki, K., Carvalho-Oliveira, R., Matsuda, M., Junqueira, M. de S., Teodoro, W. R., Vasconcellos, P. de C., Pereira, D. C. de A., Conceição, P. R. da, Saldiva, P. H. N., Mauad, T., & Macchione, M. (2020). Nrf2 positively regulates autophagy antioxidant response in human bronchial epithelial cells exposed to diesel exhaust particles. *Scientific Reports*, *10*(1), 3704. https://doi.org/10.1038/s41598-020-59930-3
25. García-Díaz, M., Birch, D., Wan, F., & Nielsen, H. M. (2018). The role of mucus as an invisible cloak to transepithelial drug delivery by nanoparticles. *Advanced Drug Delivery Reviews*, *124*, 107-124. https://doi.org/10.1016/j.addr.2017.11.002
26. Geiser, M., & Kreyling, W. G. (2010). Deposition and biokinetics of inhaled nanoparticles. *Particle and Fibre Toxicology*, *7*(1), 2. https://doi.org/10.1186/1743-8977-7-2
27. Ghio, A. J., Dailey, L. A., Soukup, J. M., Stonehuerner, J., Richards, J. H., & Devlin, R. B. (2013). Growth of human bronchial epithelial cells at an air-liquid interface alters the response to particle exposure. *Particle and Fibre Toxicology*, *10*(1), 25. https://doi.org/10.1186/1743-8977-10-25
28. Hatem, E., El Banna, N., & Huang, M.-E. (2017). Multifaceted Roles of Glutathione and Glutathione-Based Systems in Carcinogenesis and Anticancer Drug Resistance. *Antioxidants & Redox Signaling*, *27*(15), 1217-1234. https://doi.org/10.1089/ars.2017.7134
29. Hemmilä, M., Hihkiö, M., Kasanen, J.-P., Turunen, M., Hautamäki, M., Pasanen, A.-L., & Linnainmaa, K. (2007). In Vivo and In Vitro Evaluation of the Acute Toxicity, the Genotoxicity, and the Irritation Potency of Two Hexachloroethane-based Pyrotechnic Smokes. *Journal of Toxicology and Environmental Health, Part A*, *70*(14), 1167-1181. https://doi.org/10.1080/15287390701252691
30. Hemmilä, M., Hihkiö, M., Kasanen, J.-P., Turunen, M., Järvelä, M., Suhonen, S., Pasanen, A.-L., & Norppa, H. (2010). Cytotoxicity and genotoxicity in vitro and irritation potency in vivo of two red phosphorus-based pyrotechnic smokes. *Mutation Research/Genetic Toxicology and Environmental Mutagenesis*, *701*(2), 137-144. https://doi.org/10.1016/j.mrgentox.2010.06.007
31. Hemmilä, M., Hihkiö, M., & Linnainmaa, K. (2007). Evaluation of the Acute Toxicity and Genotoxicity of Orange, Red, Violet and Yellow Pyrotechnic Smokes In Vitro. *Propellants, Explosives, Pyrotechnics*, *32*(5), 415-422. https://doi.org/10.1002/prep.200700046

32. Hemmilä, M., Hihkiö, M., Norppa, H., Suhonen, S., & Callaway, J. (2013). *Toxicity assessment of signalling smokes*. 39th International Pyrotechnics Seminar, Valencia.
33. Hickey, C., Gordon, C., Galdanes, K., Blaustein, M., Horton, L., Chillrud, S., Ross, J., Yinon, L., Chen, L. C., & Gordon, T. (2020). Toxicity of particles emitted by fireworks. *Particle and Fibre Toxicology*, *17*(1), 28. https://doi.org/10.1186/s12989-020-00360-4
34. Holmes, P. S. (1999). Pneumomediastinum associated with inhalation of white smoke. *Military Medicine*, *164*(10), 751-752.
35. Ighodaro, O. M., & Akinloye, O. A. (2018). First line defence antioxidants-superoxide dismutase (SOD), catalase (CAT) and glutathione peroxidase (GPX) : Their fundamental role in the entire antioxidant defence grid. *Alexandria Journal of Medicine*, *54*(4), 287-293. https://doi.org/10.1016/j.ajme.2017.09.001
36. Jin, L., Xie, J., Wong, C. K. C., Chan, S. K. Y., Abbaszade, G., Schnelle-Kreis, J., Zimmermann, R., Li, J., Zhang, G., Fu, P., & Li, X. (2019). Contributions of City-Specific Fine Particulate Matter ($PM_{2.5}$) to Differential *In Vitro* Oxidative Stress and Toxicity Implications between Beijing and Guangzhou of China. *Environmental Science & Technology*, *53*(5), 2881-2891. https://doi.org/10.1021/acs.est.9b00449
37. Jin, X., Xue, B., Zhou, Q., Su, R., & Li, Z. (2018). Mitochondrial damage mediated by ROS incurs bronchial epithelial cell apoptosis upon ambient $PM_{2.5}$ exposure. *The Journal of Toxicological Sciences*, *43*(2), 101-111. https://doi.org/10.2131/jts.43.101
38. Juarez Facio, A. T., Yon, J., Corbière, C., Rogez-Florent, T., Castilla, C., Lavanant, H., Mignot, M., Devouge-Boyer, C., Logie, C., Chevalier, L., Vaugeois, J.-M., & Monteil, C. (2022). Toxicological impact of organic ultrafine particles (UFPs) in human bronchial epithelial BEAS-2B cells at air-liquid interface. *Toxicology in Vitro*, *78*, 105258. https://doi.org/10.1016/j.tiv.2021.105258
39. Juarez-Facio, A. T., Castilla, C., Corbière, C., Lavanant, H., Afonso, C., Morin, C., Merlet-Machour, N., Chevalier, L., Vaugeois, J.-M., Yon, J., & Monteil, C. (2022). Development of a standardized in vitro approach to evaluate microphysical, chemical, and toxicological properties of combustion-derived fine and ultrafine particles. *Journal of Environmental Sciences*, *113*, 104-117. https://doi.org/10.1016/j.jes.2021.06.001
40. Juarez-Facio, A. T., Martin de Lagarde, V., Monteil, C., Vaugeois, J.-M., Corbiere, C., & Rogez-Florent, T. (2021). Validation of a Fast and Simple HPLC-UV Method for the Quantification of Adenosine Phosphates in Human Bronchial Epithelial Cells. *Molecules*, *26*(20), 6324. https://doi.org/10.3390/molecules26206324
41. Karlsson, N., Fängmark, I., Häggqvist, I., Karlsson, B., Rittfeldt, L., & Marchner, H. (1991). Mutagenicity testing of condensates of smoke from titanium dioxide/hexachloroethane and zinc/hexachloroethane pyrotechnic mixtures. *Mutation Research/Genetic Toxicology*, *260*(1), 39-46. https://doi.org/10.1016/0165-1218(91)90078-Z
42. Kelly, F. J., & Fussell, J. C. (2015). Linking ambient particulate matter pollution effects with oxidative biology and immune responses : Oxidative stress, inflammation, and particulate matter toxicity.

Annals of the New York Academy of Sciences, *1340*(1), 84-94. https://doi.org/10.1111/nyas.12720

43. Kosanke, K. L., Kosanke, B. J., Sturman, B., Shimizu, T., Wilson, M., von Maltiz, I., Hancox, R., Kubota, N., Jennings-White, C., Chapman, D., Dillehay, D. R., Smith, T., & Podlesak, M. (2013). *Pyrotechnic Chemistry* (Journal of Pyrotechnics Inc). http://www.jpyro.com
44. Kwon, H.-S., Ryu, M. H., & Carlsten, C. (2020). Ultrafine particles : Unique physicochemical properties relevant to health and disease. *Experimental & Molecular Medicine*, *52*(3), 318-328. https://doi.org/10.1038/s12276-020-0405-1
45. Lan, Y., Ng, C. T., Ong, C. N., Yu, L. E., & Bay, B. H. (2021). Transcriptomic analysis identifies dysregulated genes and functional networks in human small airway epithelial cells exposed to ambient PM2.5. *Ecotoxicology and Environmental Safety*, *208*, 111702. https://doi.org/10.1016/j.ecoenv.2020.111702
46. Li, J., Li, J., Wang, G., Ho, K. F., Dai, W., Zhang, T., Wang, Q., Wu, C., Li, L., Li, L., & Zhang, Q. (2021). Effects of atmospheric aging processes on in vitro induced oxidative stress and chemical composition of biomass burning aerosols. *Journal of Hazardous Materials*, *401*, 123750. https://doi.org/10.1016/j.jhazmat.2020.123750
47. Li, N., Sioutas, C., Cho, A., Schmitz, D., Misra, C., Sempf, J., Wang, M., Oberley, T., Froines, J., & Nel, A. (2003). Ultrafine particulate pollutants induce oxidative stress and mitochondrial damage. *Environmental Health Perspectives*, *111*(4), 455-460. https://doi.org/10.1289/ehp.6000
48. Lin, C.-H., Lung, S.-C. C., Chen, Y.-C., & Wang, L.-C. (2021). Pulmonary toxicity of actual alveolar deposition concentrations of ultrafine particulate matters in human normal bronchial epithelial cell. *Environmental Science and Pollution Research*, *28*(36), 50179-50187. https://doi.org/10.1007/s11356-021-14265-y
49. Livak, K. J., & Schmittgen, T. D. (2001). Analysis of Relative Gene Expression Data Using Real-Time Quantitative PCR and the 2−ΔΔCT Method. *Methods*, *25*(4), 402-408. https://doi.org/10.1006/meth.2001.1262
50. Loboda, A., Damulewicz, M., Pyza, E., Jozkowicz, A., & Dulak, J. (2016). Role of Nrf2/HO-1 system in development, oxidative stress response and diseases : An evolutionarily conserved mechanism. *Cellular and Molecular Life Sciences*, *73*(17), 3221-3247. https://doi.org/10.1007/s00018-016-2223-0
51. Longhin, E., Pezzolato, E., Mantecca, P., Holme, J. A., Franzetti, A., Camatini, M., & Gualtieri, M. (2013). Season linked responses to fine and quasi-ultrafine Milan PM in cultured cells. *Toxicology in Vitro*, *27*(2), 551-559. https://doi.org/10.1016/j.tiv.2012.10.018
52. Macaulay, M. B., & Mant, A. K. (1964). SMOKE-BOMB POISONING. A FATAL CASE FOLLOWING THE INHALATION OF ZINC CHLORIDE SMOKE. *Journal of the Royal Army Medical Corps*, *110*, 27-32.
53. Martin de Lagarde, V., Rogez-Florent, T., Cazier, F., Dewaele, D., Cazier-Dennin, F., Ollivier, A., Janona, M., Achard, S., André, V., Monteil, C., & Corbière, C. (2022). Oxidative potential and in vitro toxicity of particles generated by pyrotechnic smokes in human small airway epithelial cells. *Ecotoxicology and Environmental Safety*, *239*, 113637. https://doi.org/10.1016/j.ecoenv.2022.113637

54. Merk, R., Heßelbach, K., Osipova, A., Popadić, D., Schmidt-Heck, W., Kim, G.-J., Günther, S., Piñeres, A. G., Merfort, I., & Humar, M. (2020). Particulate Matter (PM2.5) from Biomass Combustion Induces an Anti-Oxidative Response and Cancer Drug Resistance in Human Bronchial Epithelial BEAS-2B Cells. *International Journal of Environmental Research and Public Health*, *17*(21), 8193. https://doi.org/10.3390/ijerph17218193
55. National Research Council (U.S.). (1997). *Toxicity of Military Smokes and Obscurants : Volume 1* (p. 5582). National Academy Press. https://doi.org/10.17226/5582
56. National Research Council (U.S.) (Éd.). (1999). *Toxicity of Military Smokes and Obscurants : Volume 3* (p. 9645). National Academies Press. https://doi.org/10.17226/9645
57. Niu, B.-Y., Li, W.-K., Li, J.-S., Hong, Q.-H., Khodahemmati, S., Gao, J.-F., & Zhou, Z.-X. (2020). Effects of DNA Damage and Oxidative Stress in Human Bronchial Epithelial Cells Exposed to PM2.5 from Beijing, China, in Winter. *International Journal of Environmental Research and Public Health*, *17*(13), 4874. https://doi.org/10.3390/ijerph17134874
58. Paz, H. B., Tisdale, A. S., Danjo, Y., Spurr-Michaud, S. J., Argüeso, P., & Gipson, I. K. (2003). The role of calcium in mucin packaging within goblet cells. *Experimental Eye Research*, *77*(1), 69-75. https://doi.org/10.1016/S0014-4835(03)00084-8
59. Peixoto, M. S., de Oliveira Galvão, M. F., & Batistuzzo de Medeiros, S. R. (2017). Cell death pathways of particulate matter toxicity. *Chemosphere*, *188*, 32-48. https://doi.org/10.1016/j.chemosphere.2017.08.076
60. Pettilä, V., Takkunen, O., & Tukiainen, P. (2000). Zinc chloride smoke inhalation : A rare cause of severe acute respiratory distress syndrome. *Intensive Care Medicine*, *26*(2), 215-217. https://doi.org/10.1007/s001340050049
61. Platel, A., Privat, K., Talahari, S., Delobel, A., Dourdin, G., Gateau, E., Simar, S., Saleh, Y., Sotty, J., Antherieu, S., Canivet, L., Alleman, L.-Y., Perdrix, E., Garçon, G., Denayer, F. O., Lo Guidice, J. M., & Nesslany, F. (2020). Study of in vitro and in vivo genotoxic effects of air pollution fine (PM2.5-0.18) and quasi-ultrafine (PM0.18) particles on lung models. *Science of The Total Environment*, *711*, 134666. https://doi.org/10.1016/j.scitotenv.2019.134666
62. Rayner, R. E., Makena, P., Prasad, G. L., & Cormet-Boyaka, E. (2019). Optimization of Normal Human Bronchial Epithelial (NHBE) Cell 3D Cultures for in vitro Lung Model Studies. *Scientific Reports*, *9*(1), 500. https://doi.org/10.1038/s41598-018-36735-z
63. Sethi, G. S., Dharwal, V., & Naura, A. S. (2019). Immunological Basis of Oxidative Stress-Induced Lung Inflammation in Asthma and COPD. In S. Chakraborti, T. Chakraborti, S. K. Das, & D. Chattopadhyay (Éds.), *Oxidative Stress in Lung Diseases* (p. 195-223). Springer Singapore. https://doi.org/10.1007/978-981-13-8413-4_11
64. Skuland, T. S., Refsnes, M., Magnusson, P., Oczkowski, M., Gromadzka-Ostrowska, J., Kruszewski, M., Mruk, R., Myhre, O., Lankoff, A., & Øvrevik, J. (2017). Proinflammatory effects of diesel exhaust particles from moderate blend concentrations of 1st and 2nd generation biodiesel in BEAS-2B

bronchial epithelial cells—The FuelHealth project. *Environmental Toxicology and Pharmacology*, *52*, 138-142. https://doi.org/10.1016/j.etap.2017.04.004

65. Sotty, J., Garçon, G., Denayer, F.-O., Alleman, L.-Y., Saleh, Y., Perdrix, E., Riffault, V., Dubot, P., Lo-Guidice, J.-M., & Canivet, L. (2019). Toxicological effects of ambient fine (PM2.5-0.18) and ultrafine (PM0.18) particles in healthy and diseased 3D organo-typic mucocilary-phenotype models. *Environmental Research*, *176*, 108538. https://doi.org/10.1016/j.envres.2019.108538
66. Steenhof, M., Gosens, I., Strak, M., Godri, K. J., Hoek, G., Cassee, F. R., Mudway, I. S., Kelly, F. J., Harrison, R. M., Lebret, E., Brunekreef, B., Janssen, N. A., & Pieters, R. H. (2011). In vitro toxicity of particulate matter (PM) collected at different sites in the Netherlands is associated with PM composition, size fraction and oxidative potential—The RAPTES project. *Particle and Fibre Toxicology*, *8*(1), 26. https://doi.org/10.1186/1743-8977-8-26
67. Terzano, C., Di Stefano, F., Conti, V., Graziani, E., & Petroianni, A. (2010). Air pollution ultrafine particles : Toxicity beyond the lung. *European Review for Medical and Pharmacological Sciences*, *14*(10), 809-821.
68. Valavanidis, A., Vlachogianni, T., Fiotakis, K., & Loridas, S. (2013). Pulmonary Oxidative Stress, Inflammation and Cancer : Respirable Particulate Matter, Fibrous Dusts and Ozone as Major Causes of Lung Carcinogenesis through Reactive Oxygen Species Mechanisms. *International Journal of Environmental Research and Public Health*, *10*(9), 3886-3907. https://doi.org/10.3390/ijerph10093886
69. van Hulst, M., de Klerk, W. P. C., Langenberg, J. P., Tuinman, I. L., & Alblas, M. J. (2013, mai 27). *The effects of smoke hand grenades on human lung cells and bacteria for toxicity screening purposes*. 39th International Pyrotechnic Seminar, Valencia, Spain.
70. van Hulst, M., Langenberg, J. P., de Klerk, W. P. C., & Alblas, M. J. (2017). Acute Toxicity Resulting from Human Exposures to Military Smokes. *Propellants, Explosives, Pyrotechnics*, *42*(1), 17-23. https://doi.org/10.1002/prep.201600223
71. Xiao, G. G., Wang, M., Li, N., Loo, J. A., & Nel, A. E. (2003). Use of Proteomics to Demonstrate a Hierarchical Oxidative Stress Response to Diesel Exhaust Particle Chemicals in a Macrophage Cell Line. *Journal of Biological Chemistry*, *278*(50), 50781-50790. https://doi.org/10.1074/jbc.M306423200
72. Xu, F., Shi, X., Qiu, X., Jiang, X., Fang, Y., Wang, J., Hu, D., & Zhu, T. (2020). Investigation of the chemical components of ambient fine particulate matter (PM2.5) associated with in vitro cellular responses to oxidative stress and inflammation. *Environment International*, *136*, 105475. https://doi.org/10.1016/j.envint.2020.105475
73. Zhao, C., Wang, Y., Su, Z., Pu, W., Niu, M., Song, S., Wei, L., Ding, Y., Xu, L., Tian, M., & Wang, H. (2020). Respiratory exposure to PM2.5 soluble extract disrupts mucosal barrier function and promotes the development of experimental asthma. *Science of The Total Environment*, *730*, 139145. https://doi.org/10.1016/j.scitotenv.2020.139145

74. Zheng, F., Gonçalves, F. M., Abiko, Y., Li, H., Kumagai, Y., & Aschner, M. (2020). Redox toxicology of environmental chemicals causing oxidative stress. *Redox Biology*, *34*, 101475. https://doi.org/10.1016/j.redox.2020.101475

Figures

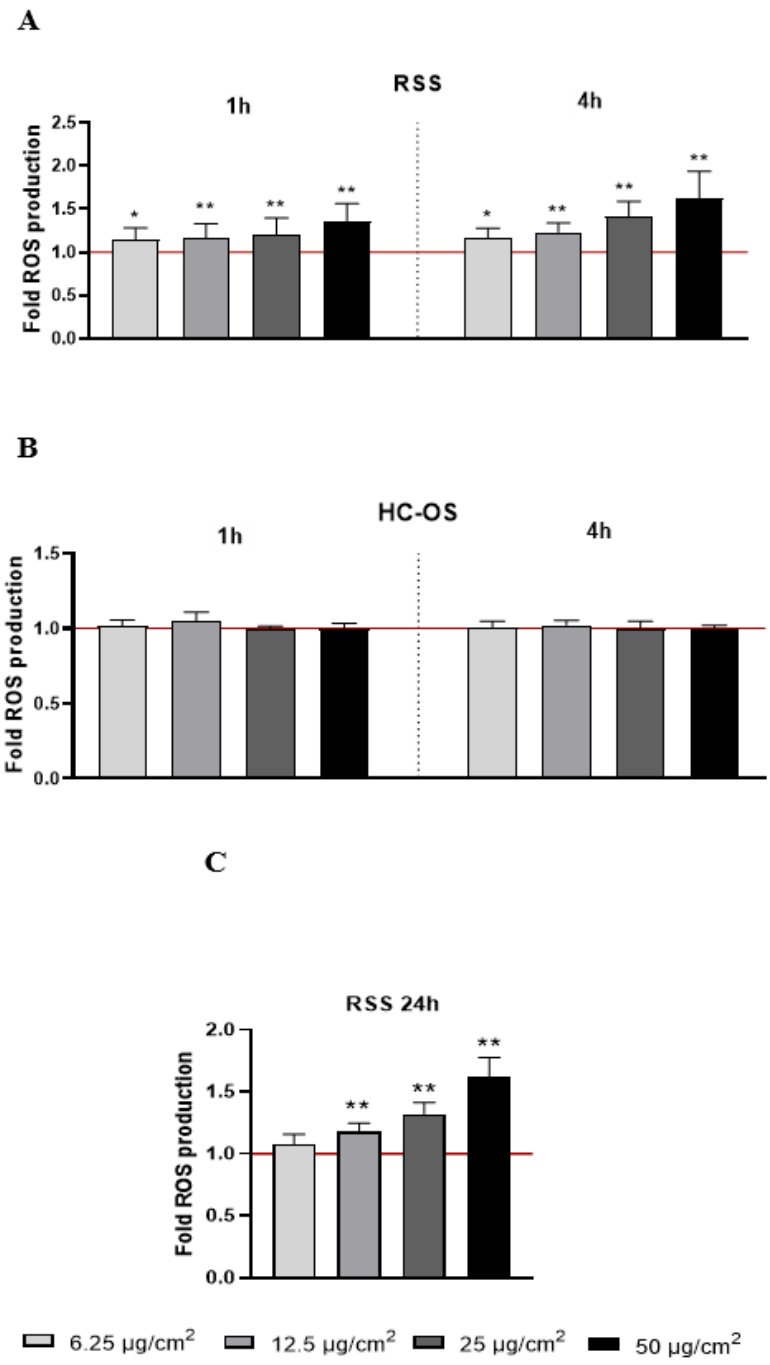

Figure 1

ROS production measured by MitoSox probe. 3D NHBE cells were exposed 1 h and 4 h to RSS (A) and HC-OS particles (B) and 24 h to RSS particles (C). Results are presented as ratio of fluorescence signal compared to control (cells cultured with PBS). Data were expressed as mean value ± SD ($n \geq 3$). *$p \leq 0.05$, ** $p \leq 0.01$.

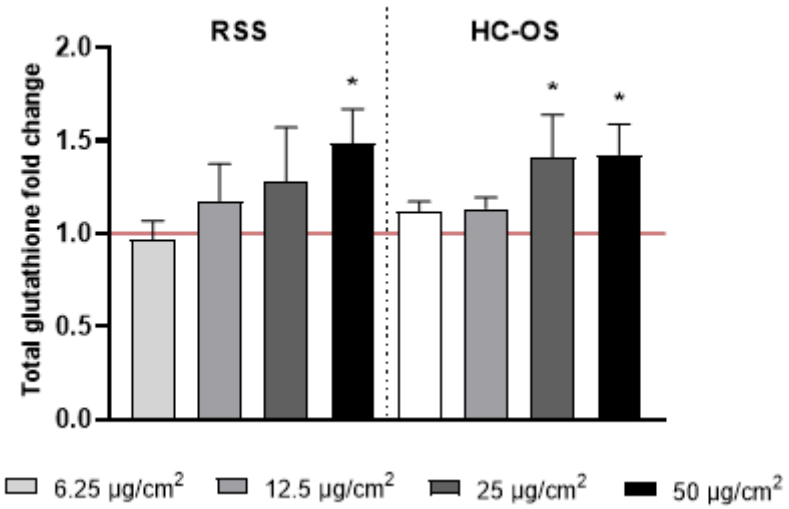

Figure 2

Total glutathione level after 24 h of exposure to RSS or HC-OS particles (6.25, 12.5, 25, 50 µg/cm^2). Results are presented as ratio of concentration of total glutathione compared to control (cells cultured with PBS). Data were expressed as mean value ± SD ($n \geq 3$). *$p \leq 0.05$

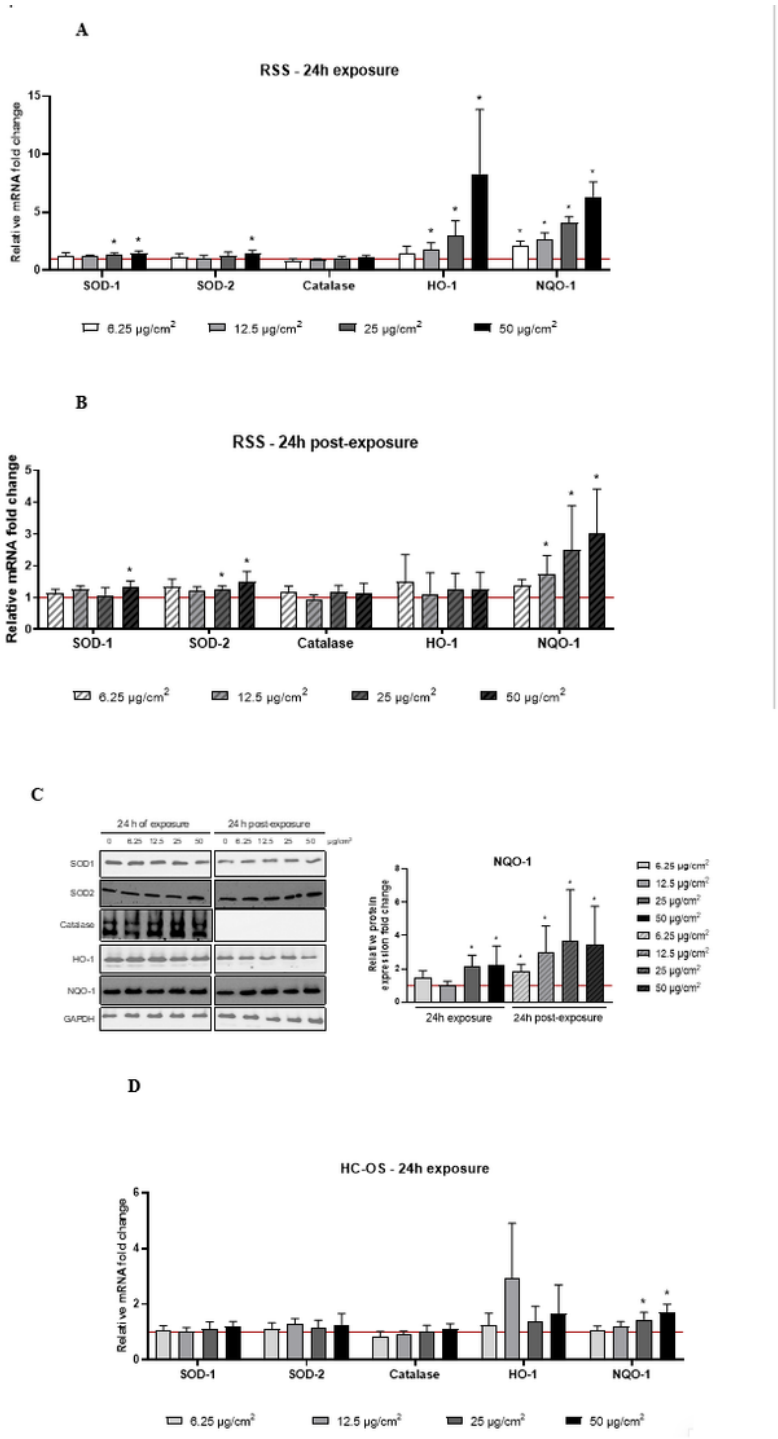

Figure 3

Antioxidant mRNA expression after 24 h of exposure (A) to RSS particles and 24 h post-exposure (B) (6.25, 12.5, 25, 50 µg/cm^2). Antioxidant protein levels after 24 h of exposure to RSS particles and 24 h post-exposure (6.25, 12.5, 25, 50 µg/cm^2) (C), representative western blot obtained from cropping blots images (Right) and relative quantification of NQO-1 protein level (Left). Antioxidant mRNA expression after 24 h of exposure to HC-OS particles (6.25, 12.5, 25, 50 µg/cm^2) (D). SOD-1 and -2, superoxide

dismutases-1 and -2 ; NQO-1, NADPH quinone oxydoreductase-1 ; HO-1, heme oxygenase-1. Results are presented as ratio of signal compared to control (cells cultured with PBS). Data were expressed as mean value ± SD of ($n \geq 3$). *$p \leq 0.05$.

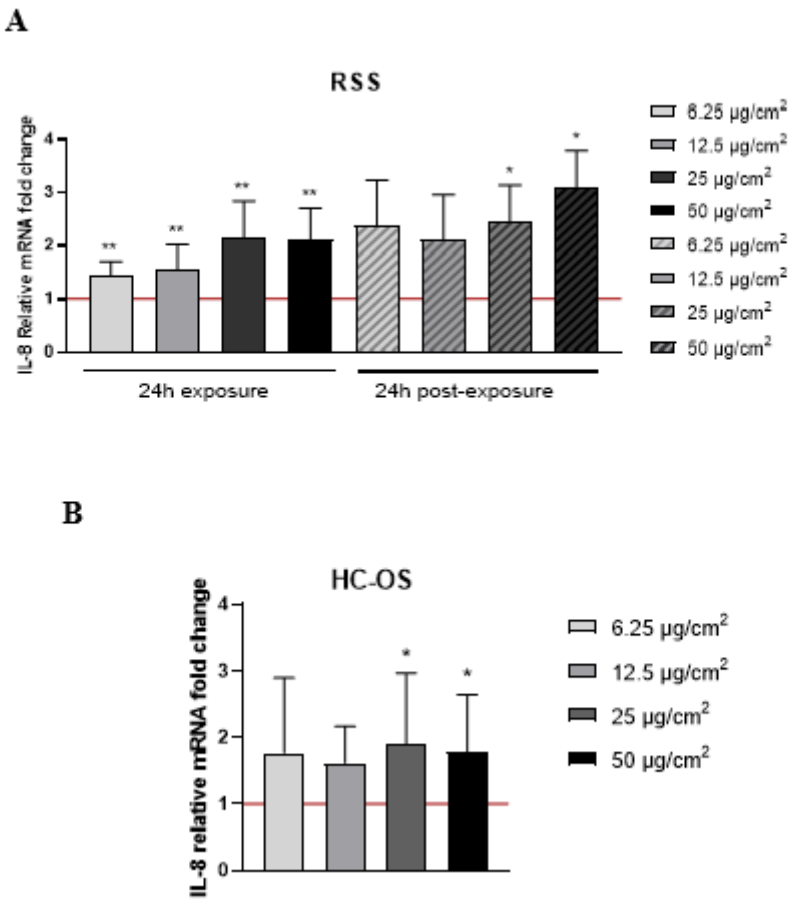

Figure 4

IL-8 mRNA expression after 24 h of exposure to RSS particles and 24 h post-exposure (6.25, 12.5, 25, 50 µg/cm^2) (**A**); IL-8 mRNA expression after 24 h of exposure to HC-OS particles (6.25, 12.5, 25, 50 µg/cm^2) (**B**),.Results are presented as ratio of signal compared to control (cells cultured with PBS). Data were expressed as mean value ± SD ($n \geq 3$). *$p \leq 0.05$, **$p \leq 0.01$

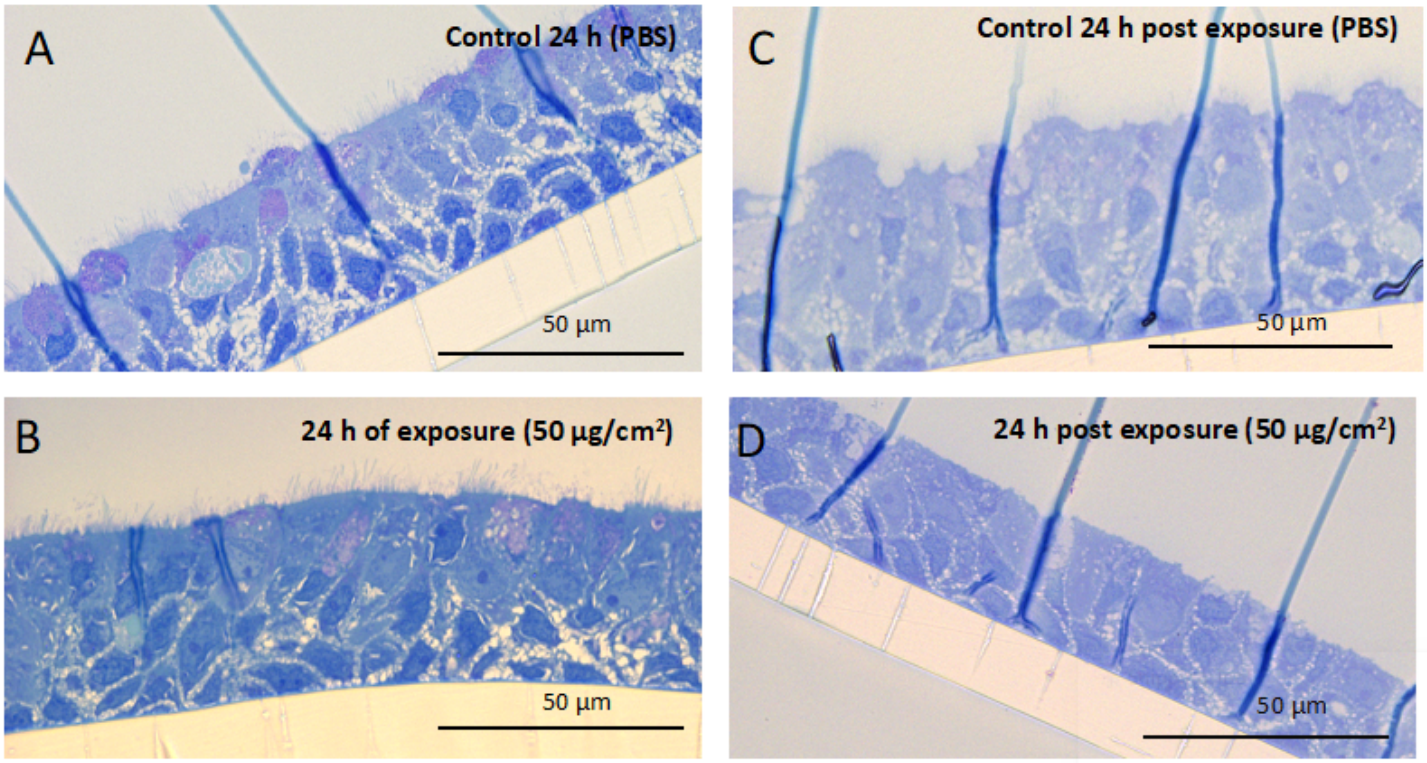

Figure 5

Phenotype of 3D NHBE cells after RSS exposure. A-C : Control with PBS buffer; B: 24 h of exposure to RSS particles (50 µg/cm^2), D: 24 h post-exposure (50 µg/cm^2). Scale bar: 50µm

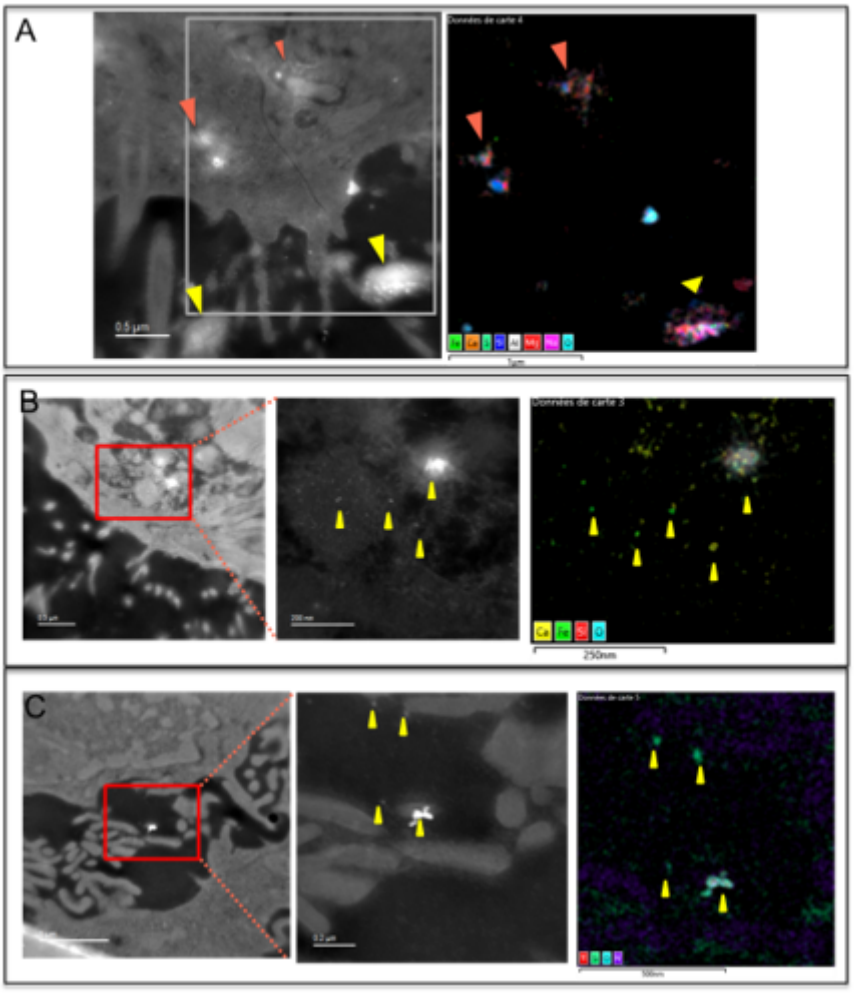

Figure 6

Fate of particles after 24 h of exposure to RSS particles at 50 µg/cm^2. Black &white micrograph are acquired in STEM-HAADF mode allowing, in electron microscopy, the detection of particles with high atomic mass as brighter contrast than the biological matrix. Colored images represent the chemical maps of elemental compound presents in the cells obtained by STEM-EDS **A**: Apex of epithelium showing ciliated cells with intercellular space and microvilli. Sub-micron particles are trapped outside the epithelium in the mucus (yellow arrows) while smaller aggregates are found inside (Red arrows). **B**: Apex of epithelium with microvilli in the luminal space. Nanoranged particles are internalized in apical cells as small cluster or single particles enriched in Fe. **C**: Basal cells of the epithelium. We notice the presence of nanoranged particles containing Fe, Si trapped in the intercellular space between two basal cells.

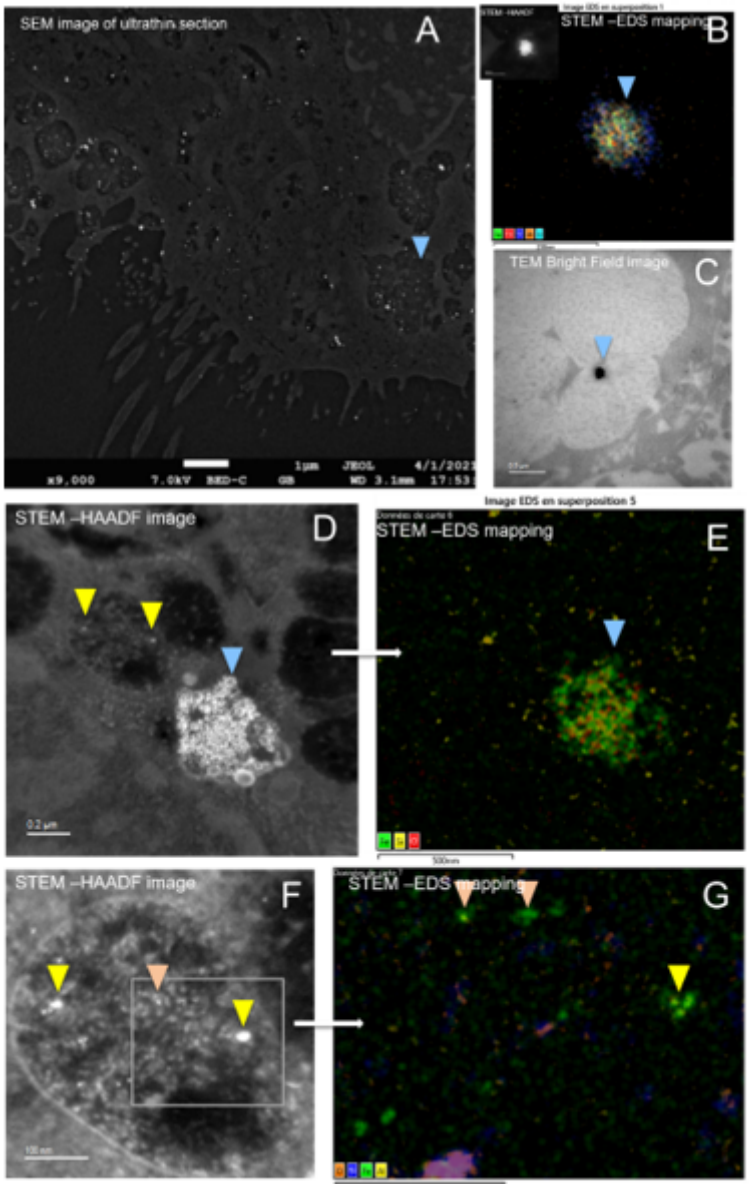

Figure 7

24 h post-exposure of 3D NHBE cells to RSS particles: Combined electron microscopy approach using SEM and (S)TEM-analysis **A**: SEM images obtained with backscattered electrons detector giving an overview of the presence of heavy elements in 3D NHBE cells (Bright dots). **C-F**: Transmission electron microscopy in mode bright field (**C**), STEM-HAADF (**D-F**). **B-E-G**: STEM-EDS elemental qualitative mapping showing the distribution of particles into cells. Particles which contain Fe, Al, Ca, Si, O (chemical compounds of RSS) are internalized in large intracytoplasmic compartments, and seems to be associated with mucin.

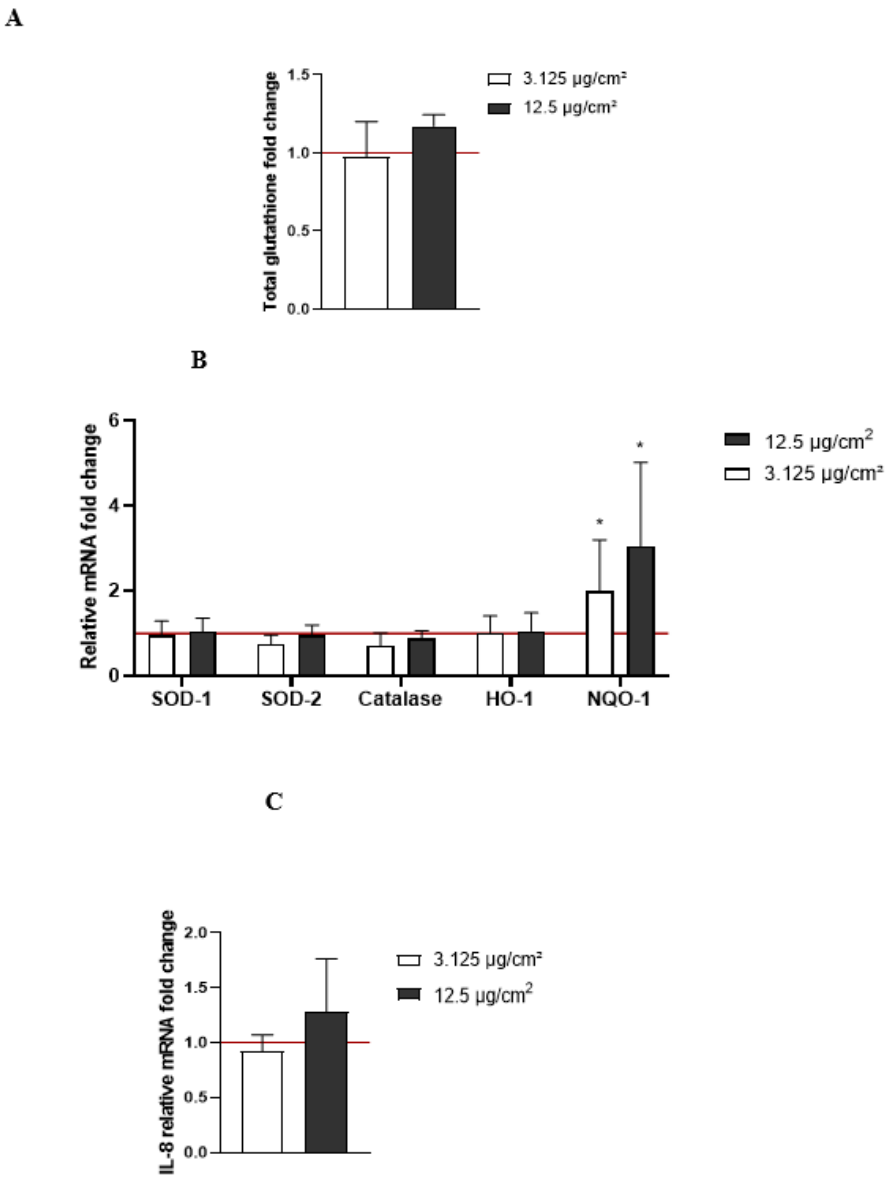

Figure 8

Total glutathione (**A**), antioxidant mRNA expression (**B**) and *IL-8* mRNA expression (**C**) after four treatments of 16 h to RSS (3.125 ; 12.5 µg/cm^2). Results are presented as ratio of signal compared to control (cells cultured with PBS). Data were expressed as mean value ± SD (n ≥ 3). *p ≤ 0.05.

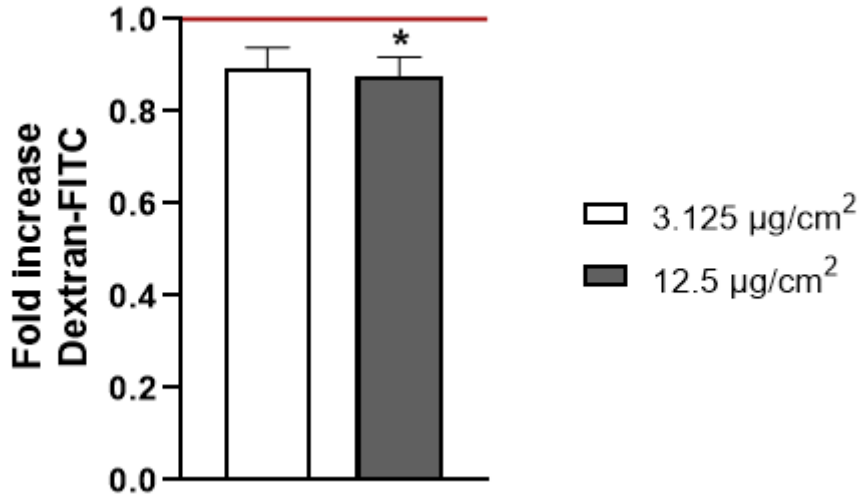

Figure 9

Epithelium barrier permeability analysis using Dextran-FITC assay. 3D NHBE cells were submitted to four treatments of 16 h to RSS particles (3.125 ; 12.5 µg/cm^2). Results are presented as ratio of fluorescence signal compared to control (cells cultured with PBS). Data were expressed as mean value ± SD (n ≥ 3). *p ≤ 0.05

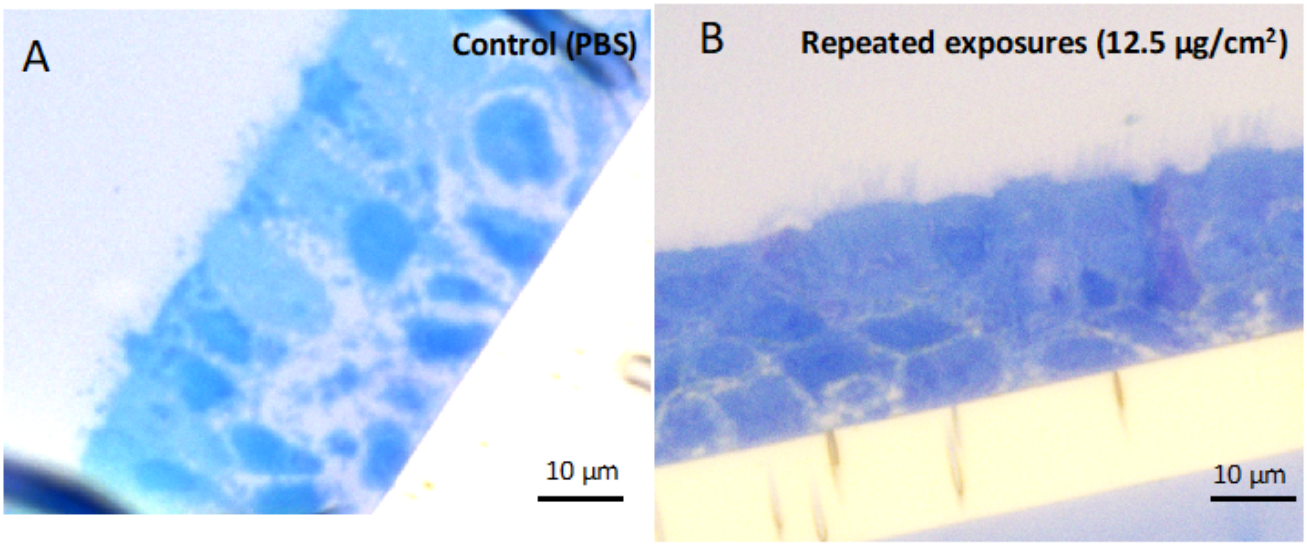

Figure 10

Phenotype of 3D NHBE cells after RSS exposure. A: Control with PBS buffer; B: Repeated exposure (12.5µg/cm^2) scale bar: 10µm

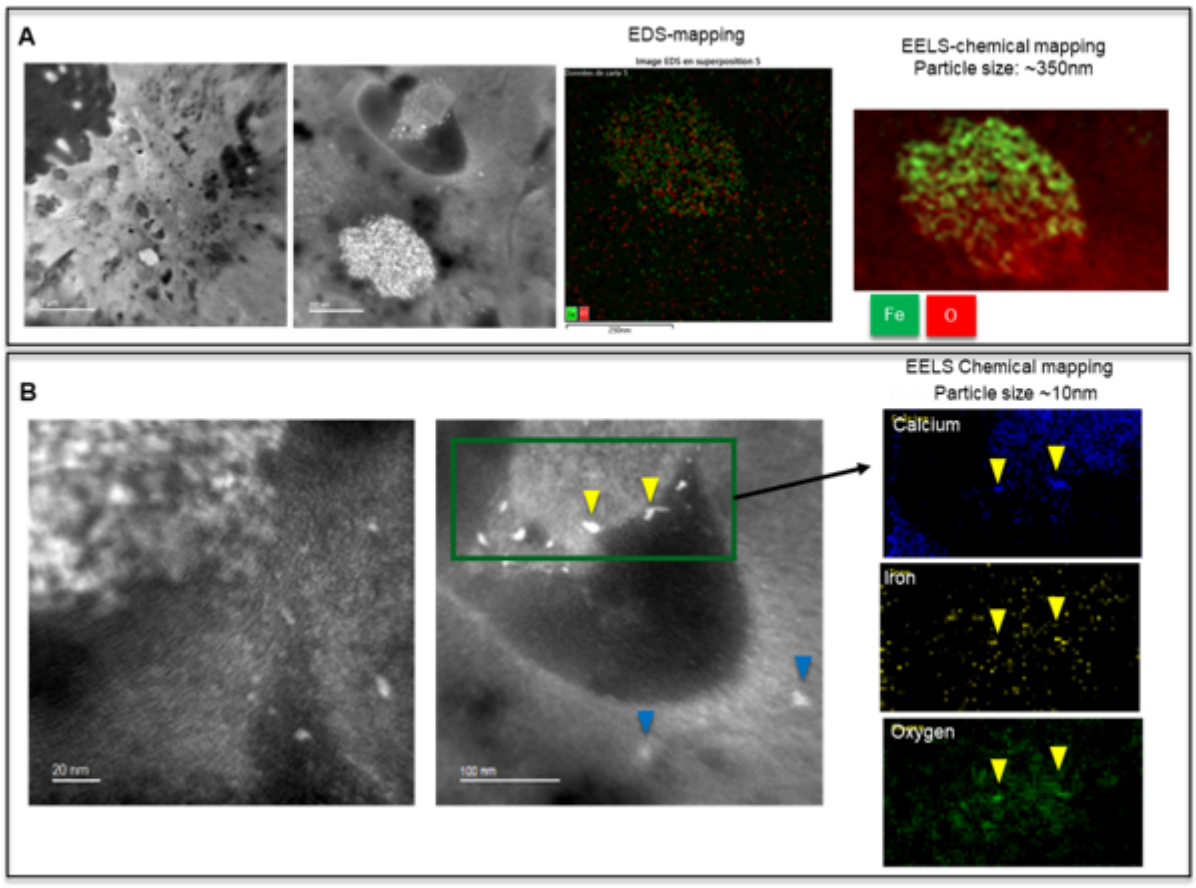

Figure 11

Distribution analysis of RSS particles in the 3D NHBE cells after repeated exposure showing the persistence of particle into the cells. **A**: Accumulation of nanometric particles in intracytoplasmic compartments, forming large aggregates (~350nm), whose chemical nature Fe-O is confirmed by EDS and energy loss (EELS) mappings. **B**: presence of isolated nanoparticles (10 nm) having diffused into the cytoplasm (blue arrows) or interacting with the membrane of vacuolar compartments (yellow arrows). The chemical nature of the particles is difficult to identify and tends to reveal the presence of Fe, O, Ca.

Supplementary Files

This is a list of supplementary files associated with this preprint. Click to download.

- SuppData.docx